Cell Biology

The Rab7-Epg5 and Rab39-ema modules cooperately position autophagosomes for efficient lysosomal fusions

Reviewed Preprint
v1 • November 7, 2024
Not revised

Attila Boda, Villő Balázs, Anikó Nagy, Dávid Hargitai, Mónika Lippai, Zsófia Simon-Vecsei, Márton Molnár, Fanni Fürstenhoffer, Gábor Juhász, Péter Lőrincz

Department of Anatomy, Cell and Developmental Biology, Eötvös Loránd University, Budapest, Hungary • HAS-ELTE Momentum Vesicular Transport Research Group, Hungarian Academy of Sciences & ELTE Eötvös Loránd University, Budapest, Hungary • Lysosomal Degradation Research Group, Institute of Genetics, HUN-REN BRC Szeged, Szeged, Hungary

https://en.wikipedia.org/wiki/Open_access
Copyright information

eLife Assessment

This paper presents **valuable** findings on how autophagosomes are positioned along microtubules for their efficient fusion with lysosomes, providing significant insights into the mechanism. The evidence supporting the conclusions is **solid**, with high-quality fluorescence microscopy combined with Drosophila genetics. This work will be of broad interest to cell biologists interested in autophagy and related cell biology fields.

https://doi.org/10.7554/eLife.102663.1.sa3

Abstract

Macroautophagy, a major self-degradation pathway in eukaryotic cells, utilizes autophagosomes to transport self-material to lysosomes for degradation. While microtubular transport is crucial for the proper function of autophagy, the exact roles of factors responsible for positioning autophagosomes remain incompletely understood. In this study, we performed a loss-of-function genetic screen targeting genes potentially involved in microtubular motility. A genetic background that blocks autophagosome-lysosome fusions was used to accurately analyze autophagosome positioning. We discovered that pre-fusion autophagosomes move towards the non-centrosomal microtubule organizing center (ncMTOC) in *Drosophila* fat cells, which requires a dynein-dynactin complex. This process is regulated by the small GTPases Rab7 and Rab39 together with their adaptors: Epg5 and ema, respectively. The dynein-dependent movement of vesicles toward the nucleus/ncMTOC is essential for efficient autophagosomal fusions with lysosomes and subsequent degradation. Remarkably, altering the balance of kinesin and dynein motors changes the direction of autophagosome movement, indicating a competitive relationship where normally dynein-mediated transport prevails. Since pre-fusion lysosomes were positioned similarly to

autophagosomes, it indicates that pre-fusion autophagosomes and lysosomes converge at the ncMTOC, which increases the efficiency of vesicle fusions.

Introduction

Macroautophagy is an essential self-degradation pathway in eukaryotic cells, during which double-membrane-bound autophagosomes transport materials to lysosomes for degradation (Parzych & Klionsky, 2014). Defects in autophagy are associated with multiple pathologies, prompting extensive study of its molecular players over the past decades (Lei & Klionsky, 2021). During macroautophagy, a double-membrane structure called an autophagosome is formed in an *atg* gene-dependent manner. This autophagosome then fuses with a lysosome or late endosome in a process dependent on the small GTPases Rab7, Rab2, and Arl8, the HOPS tethering complex, and the SNARE proteins Syntaxin17, Ubisnap/SNAP29, and Vamp7 (Lőrincz & Juhász, 2020).

Autophagosomes are suggested to form at random locations within the cytoplasm and are subsequently transported toward the cell center (Jahreiss et al., 2008; Kimura et al., 2008). Establishing proper proximity between autophagosomes and lysosomes is essential for their ability to fuse. The microtubular network and associated motor proteins are crucial for most vesicular transport. Thus, the involvement of the microtubular system has been suggested in various aspects of autophagosome dynamics, including biogenesis, transport, amphisome formation (Köchl et al., 2006), and autophagic clearance (Ravikumar et al., 2005). It is proposed that while microtubules are necessary for the maturation of autophagosomes, their fusion capacity is independent of microtubules (Fass et al., 2006). Nevertheless, dynein-regulated autophagosomal motility appears indispensable for efficient lysosomal fusion (Jahreiss et al., 2008; Kimura et al., 2008). How autophagosomes gain the ability to move along microtubules remains unclear. It is suggested that autophagic vesicles acquire dyneins by endosomal fusion (Cheng et al., 2015); however, autophagosomes still appear to be motile upon Syx17 loss (Neisch et al., 2017).

Most of our knowledge about autophagosome positioning and movement comes from studies on neurons, where autophagosomes form in the terminal part of axons and then travel toward the soma by dynein-dynactin-regulated bulk retrograde transport during basal autophagy (Ikenaka et al., 2013; Lee et al., 2011; Maday et al., 2012; Wang et al., 2015). During their route, they fuse with endosomes and lysosomes, resulting in gradual acidification and the acquisition of lysosomal markers (Hill & Colón-Ramos, 2020; Lee et al., 2011). Degradation takes place in the cell body (Maday et al., 2012). Inhibited retrograde transport leads to neurodegeneration and defective removal of synaptic autophagosomes (Fu et al., 2014; Lee et al., 2011; Ravikumar et al., 2005), highlighting the importance of axonal transport in the acidification and degradation processes.

Autophagosomes are suggested to use both dyneins and kinesins in neuronal cells. Initially, they exhibit bidirectional motility at the axon tip, later shifting to dynein-regulated retrograde transport directed toward the soma, where the already mature autolysosomes again show bidirectional motility (Maday et al., 2012). Various scaffolding proteins have been found to regulate autophagosome transport, including CKA as part of the STRIPAK complex (Neisch et al., 2017), JIP1, JIP3, and JIP4 (Cason et al., 2021; Cason & Holzbaur, 2023; Fu et al., 2014), as well as Huntingtin and HAP1 (Cason et al., 2021; Hill & Colón-Ramos, 2020; Wong & Holzbaur, 2014). It is important to note that before autophagosome closure, phagophores are not able to be transported (Fass et al., 2006).

However, most of our knowledge about autophagosome motility comes from experimental methods and tools that do not distinguish between non-acidic autophagosomes and autophagic structures that have already undergone some endolysosomal fusion and acidification. For

example, several studies used reporters such as LC3 fused to red fluorescent proteins, which also label post-fusion autolysosomes. Consequently, autophagic organelles that have acidified are sometimes still considered autophagosomes, when in fact they could be autolysosomes.

We and our colleagues have previously identified and characterized several key players in autophagosome-lysosome fusion in starved *Drosophila* fat cells (Boda et al., 2019; Hegedűs et al., 2016; Lőrincz, Tóth, et al., 2017; Takáts et al., 2013; Takáts et al., 2014). During these studies, we observed an intriguing phenomenon: despite being generated at random positions in the cytosol, autophagosomes accumulated around the nucleus when either the HOPS tethering complex or the SNARE fusion machinery was inhibited (Boda et al., 2019; Lőrincz et al., 2019; Takáts et al., 2013; Takáts et al., 2014).

This observation led us to employ a novel and unique approach by examining autophagosome positioning in cells where autophagosome-lysosome fusion was inhibited using HOPS RNAi. This method allowed us to exclude the confounding effects of ongoing vesicle fusions, which could otherwise obscure the accurate determination of the roles of different factors in vesicle positioning. These cells were utilized in an RNA interference screen to identify and characterize the molecular participants involved in autophagosome positioning. Our work represents the first comprehensive description of the transport machinery involved in pre-fusion autophagosomes and its significance during autolysosome formation.

Results

We began our investigations by performing an RNA interference screen to identify genes potentially involved in the microtubular positioning of autophagosomes, including MT proteins and motors (such as dynein, dynactin, and kinesin subunits), Rab small GTPases, and their effectors (for the complete list of tested genes and results, see Supplementary File 1 and Supplementary Table 1). We used larval fat cells of the fruit fly (*Drosophila melanogaster*) as a model system, in which bulk macroautophagy was induced by starvation (Scott et al., 2004). The fat tissue contained GFP-positive mosaic cells, in which we silenced the gene of interest together with the Vps16A central subunit of the HOPS complex. This RNAi effectively impairs autophagosomal fusion, leading to the accumulation of autophagosomes (Takáts et al., 2014). Fat cells also expressed an mCherry-Atg8a reporter driven by a *UAS*-independent fat body-specific *R4* promoter. This reporter marks both autophagosomes and autolysosomes in control cells, due to the stability of mCherry in acidic environments (**Fig. 1A**). However, in *vps16a* RNAi cells, which also expressed a control (*luciferase*) RNAi, we observed the accumulation of small mCherry-Atg8a puncta—representing autophagosomes—in the perinuclear region (**Fig. 1A, B, F**), consistent with previous observations (Takáts et al., 2014).

Similar observations were made by endogenous immunostaining against Atg8a (Fig. S1A, G), Rab7 (Fig. S1B, H), and Arl8 (Fig. S1C, I). Endogenous Atg8a immunostaining is specific for autophagosomes (Lőrincz, Mauvezin, et al., 2017), Rab7 antibody labels late endosomes, lysosomes, and autophagosomes (Hegedűs et al., 2016), while Arl8 is a lysosome-specific small GTPase responsible for lysosomal motility and autophagosome-lysosome fusion (Bagshaw et al., 2006; Boda et al., 2019; Hofmann & Munro, 2006). Our results thus indicate that cells with impaired autophagosome-lysosome fusion accumulate not only pre-fusion autophagosomes but also pre-fusion lysosomes or late endosomes around their nuclei. To confirm that our mCherry-Atg8a reporter labels structures of autophagic origin, we co-expressed an *atg8a* RNAi with *vps16a* RNAi, which effectively removed the signal of mCherry-Atg8a from the mosaic cells (Fig. S1D, J), confirming that this reporter does not label non-autophagic vacuoles in these cells. To exclude the possibility that the perinuclear accumulation of autophagosomes and unfused lysosomes is due to the overall disorganization of organelles in Vps16A-depleted cells, we immunostained the cells against Gmap, which revealed that the positions of the Golgi apparatuses remained control-like

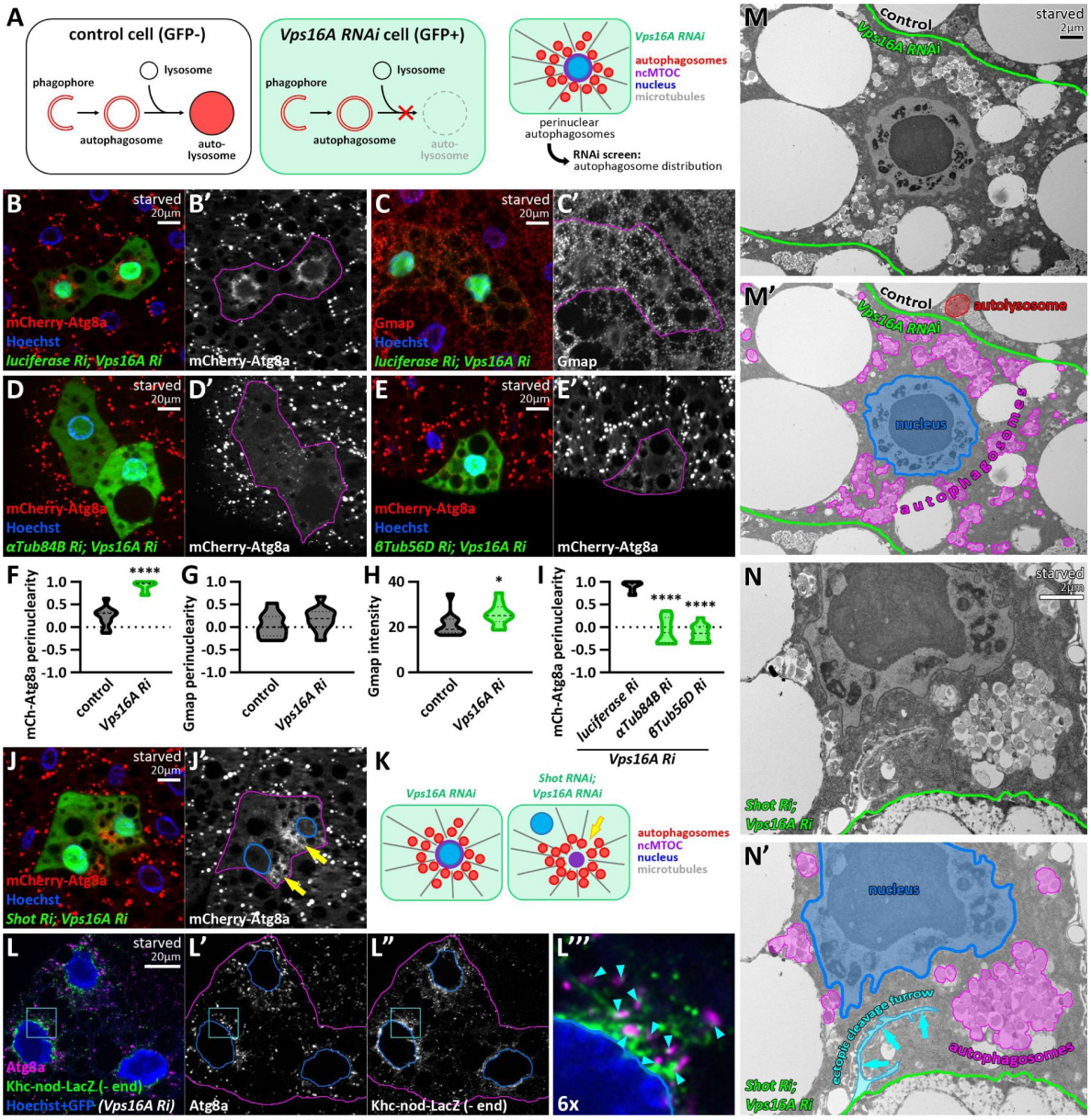

Figure 1.

Autophagosomes move towards the ncMTOC in fat cells.

A: Schematic drawing of the experimental design for screening. **B:** Non-fused autophagosomes accumulate in the perinuclear region upon Vps16A silencing. **C:** The cis-Golgi compartment remains unchanged upon the expression of *vps16a* RNAi. **D, E:** The accumulation of autophagosomes is not perinuclear in *α* or *β tubulin*; *vps16a* double RNAi cells. **F-I:** Quantification of data shown in B-E; n=10 cells. **J, K:** Autophagosomes position at an ectopic MTOC (yellow arrows) formed upon Shot silencing. (29 out of 41 cells exhibited an ectopic MTOC = 70.73%). **L:** Autophagosomes are near microtubule minus-ends, marked by Khc-nod-LacZ. The boxed area in the main panels, marked by cyan, is enlarged in L''' (proximity sites indicated by cyan arrowheads). **M, N:** Correlative ultrastructural analysis shows autophagosomes accumulating near the nucleus upon Vps16A silencing (border of control and silencing cells marked by green) (M). Shot knockdown causes aggregation of autophagosomes in ectopic foci in *vps16a* RNAi cells (N). An ectopic cleavage furrow (hallmark of Shot depletion (Sun et al., 2019)) is also visible (cyan arrows in N'). Note: the magnification of N is higher to better show this structure. Nuclei are encircled in blue in J' and L', L'''. The boundaries of RNAi cells are highlighted in magenta in the grayscale panels.

upon Vps16A silencing. Additionally, the fluorescent signal of Gmap was increased in Vps16A-depleted cells, which is consistent with the fact that the Golgi apparatus is a substrate of golgiphagy in flies (Rahman et al., 2022) (**Fig. 1C, G, H**).

The transport of autophagosomes is microtubule-dependent and minus-end directed

As microtubule (MT)-associated autophagosome transport has been suggested to be more prominent compared to the actomyosin network (Lőrincz & Juhász, 2020), we first silenced the microtubule subunits α- and β-tubulin in *vps16a* RNAi cells to clarify whether the perinuclear localization of autophagosomes is indeed established by the MT network. As expected, knockdown of tubulins diminished the perinuclear localization of autophagosomes and led to their scattering in the cytoplasm (**Fig. 1D, E, I**). Larval fat body cells have been shown to possess a perinuclear, non-centrosomal MTOC (ncMTOC) (Zheng et al., 2020). This ncMTOC is stabilized by the Spectraplakin Short stop (Shot), and its depletion translocates the perinuclear ncMTOC to an ectopic, cytosolic location (Sun et al., 2019; Zheng et al., 2020). Therefore, we hypothesized that autophagosomes travel towards this MTOC in starved fat cells, and it is the position of the ncMTOC, rather than the nucleus, that determines their direction. Accordingly, autophagosomes accumulated in a central cytosolic region rather than around the nucleus in *shot*, *vps16a* double RNAi cells (**Fig. 1J, K, S1E, F**).

To further confirm that autophagosomes indeed travel towards the ncMTOC, we expressed the MT minus-end reporter Khc-nod-LacZ (a hybrid recombinant kinesin) (Clark et al., 1997) in *vps16a* RNAi cells. Immunolabeling of Atg8a-marked autophagosomes revealed their close proximity to the reporter, which effectively labeled the perinuclear MT network (**Fig. 1L**). Additionally, we performed ultrastructural analysis to further support our findings. Compared to the mostly perinuclear distribution of autophagosomes in Vps16A single knockdown cells (**Fig. 1M**), s*hot, vps16a* double RNAi resulted in the concentration of autophagosomes in large groups adjacent to the nucleus, consistent with our fluorescent data (**Fig. 1N**). Taken together, our results indicate that autophagosomes move along the MT network oriented towards the MT minus-end to their final destination near the ncMTOC.

A cytoplasmic dynein-dynactin complex transports autophagosomes

Next, we turned to microtubular motor complex subunits. Dynein complexes consist of motor domain-containing heavy chains (HC), intermediate chains (IC), light intermediate chains (LIC), and light chains (LC), and their functions are regulated by dynactin complexes (Canty et al., 2021; Vaughan & Vallee, 1995). The fruit fly genome contains two genes encoding HCs and LICs, one single IC gene, and several genes encoding LCs. These can form several cytoplasmic dynein complexes; our goal was to find the one(s) responsible for autophagosome transport. Upon silencing Dynein heavy chain 64C (Dhc64C, a HC subunit), short wing (sw, an IC subunit), Dynein light intermediate chain (Dlic, a LIC subunit), and roadblock (robl, a LC subunit) in *vps16a*-silenced cells, we observed an interesting phenomenon: autophagosomes accumulated in the cell periphery, under the plasma membrane, and not around the nucleus (**Fig. 2A-D, K**, S2A, R). Similar to the dynein hits, the silencing of DCTN1-p150 (Dynactin 1, p150Glued homolog), DCTN2-p50, and DCTN4-p62 also resulted in the redistribution of autophagosomes to the cell periphery (**Fig. 2E-G, K**, S2B, C, R). Our mCherry-Atg8a data were strengthened by endogenous Atg8a and Rab7 immunostainings (Fig. S2D-I, T, U), as Atg8a and Rab7 positive puncta also redistributed to the cell periphery upon co-silencing Vps16A with our dynein or dynactin hits.

We also overexpressed a dominant-negative form of DCTN1-p150, as well as a wild-type DCTN2-p50/dynamitin, which is described to cause dominant-negative effects when overexpressed (Zheng et al., 2020). These reproduced the phenotypes of dynein or dynactin loss, further strengthening

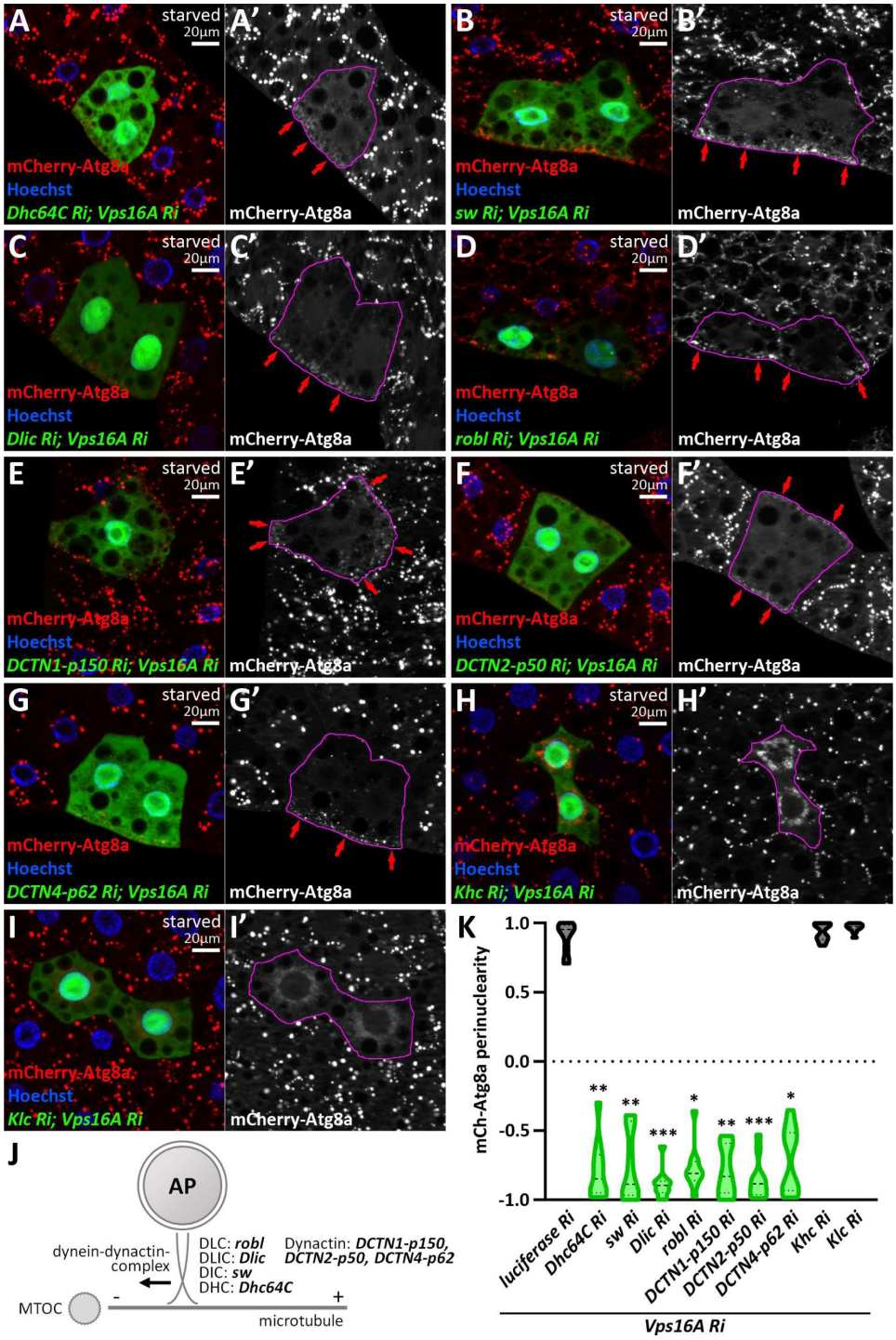

Figure 2.

A dynein-dynactin complex is required for minus-end directed autophagosome transport.

A-G: Knockdown of dynein (A-D) and dynactin subunits (E-G) results in the peripheral redistribution of autophagosomes in *vps16a* RNAi cells (red arrows). **H, I:** Kinesin silencing does not affect the perinuclear accumulation of autophagosomes in *vps16a* RNAi cells. **J:** Proposed model of the suggested dynein-dynactin complex responsible for autophagosome positioning in fat cells. DHC: dynein heavy chain; DIC: dynein intermediate chain; DLIC: dynein light intermediate chain; DLC: dynein light chain. **K:** Quantification of data shown in A-I; n=10 cells. The boundaries of RNAi cells are highlighted in magenta in the grayscale panels.

our data (Fig. S2J, K, R). In turn, silencing other dynein or dynactin genes did not cause similar effects; these cells were either control-like (*vps16a* single RNAi) (Supplementary File 1, Supplementary Table 1) or, in two cases, a mild scattering of autophagosomes were observed (Dlc90F, an LC subunit, and capping protein alpha, cpa, a dynactin subunit) (Fig. S2L, M, S, Supplementary File 1, Supplementary Table 1).

Our results thus suggest that autophagosomes are mainly transported by a cytosolic dynein complex composed of Dhc64 (HC), sw (IC), Dlic (LIC), and roadblock (LC), regulated by a DCTN1-2-4 containing dynactin complex (**Fig. 2J**). Importantly, the peripheral accumulation of autophagosomes upon the lack of dynein-regulated movement suggests that kinesins can take their place and carry autophagosomes to the positive end of microtubules.

We continued screening by silencing dynein activators and regulators. These proteins, including the Bicaudal-D, Hook, and Ninein families in mammals, are responsible for enhancing processive motility and recruiting cargo to the dynein-dynactin complex (Olenick & Holzbaur, 2019; Redwine et al., 2017). We found that the silencing of a candidate activator, Girdin (Redwine et al., 2017), in a *vps16a* RNAi background led to the dispersal of autophagosomes (Fig. S2N, V), similarly to the loss of Lis-1, a well-studied and essential regulator of dynein motor function (Dix et al., 2013; Siller et al., 2005; Sitaram et al., 2012; Swan et al., 1999) (Fig. S2O, V). This can be explained by the fact that some dynein function is still present without Girdin and Lis-1, and their loss does not completely abolish dynein activity.

Therefore, next our screen focused on kinesin motors. Importantly, none of the kinesin knockdowns inhibited or significantly enhanced the perinuclear positioning of autophagosomes in *vps16a*-depleted cells (Khc and Klc as examples are shown, **Fig. 2H, I, K, S2P, Q, T**, Supplementary File 1, Supplementary Table 1). These results suggest that cells predominantly use the dynein complex to transport autophagosomes, rather than kinesins.

A proper dynein/kinesin ratio determines the direction of autophagosome positioning

Since dynein loss leads to the peripheral relocation of autophagosomes, we hypothesized that in this case, kinesins take over the role of transporting autophagosomes, preferring the opposite direction. To examine this possibility, we overexpressed two kinesin motors (Klp67A, Klp98A) in *vps16a* RNAi cells. Strikingly, both resulted in the scattering of autophagosomes, and in some cases, caused the peripheral accumulation of mCherry-Atg8a puncta, resembling dynein loss (**Fig. 3A, B, F**). Moreover, autophagosomes scattered upon co-silencing a dynactin and a kinesin in *vps16a* RNAi cells (**Fig. 3C, F**). This suggests that without MT motors, autophagosomes are unable to move properly.

To further examine the relationship between dyneins and kinesins, we expressed the recombinant kinesin Khc-nod-LacZ in *vps16a* single and dynactin, *vps16a* double RNAi cells. This recombinant kinesin contains the cargo domain of Khc but moves towards the MT minus-end, similar to dyneins. Interestingly, overexpression of Khc-nod-LacZ in *vps16a* single RNAi cells appeared to influence the assembly and/or function of the ncMTOC, as the nuclear envelope was only partly surrounded by autophagosomes, but their distribution remained perinuclear (**Fig. 3D, F**). Strikingly, when we overexpressed this recombinant kinesin in dynactin, Vps16A double knockdown cells, autophagosomes became dispersed (**Fig. 3E, F**), and no longer accumulated at the periphery as seen in *dynactin1-p150*, *vps16a* double RNAi cells. Since kinesins do not require the activity of dynactins, this suggests that this recombinant kinesin could partially rescue the dynein/dynactin function loss and take over the role of the missing minus-end motors, further supporting that a proper dynein/kinesin ratio determines the direction of autophagosome positioning.

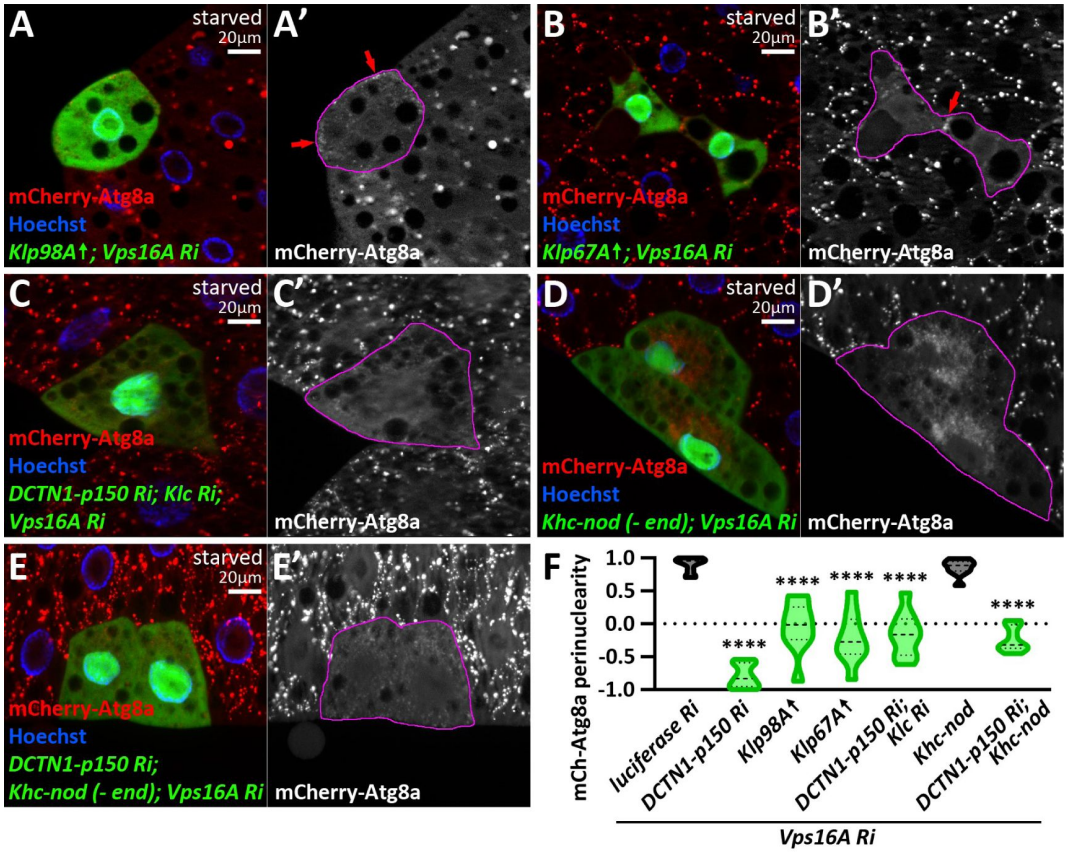

Figure 3.

The proper dynein/kinesin ratio determines the directionality of autophagosome transport.

A, B: Overexpression of kinesin motors blocks the minus-end transport of autophagosomes, leading to their accumulation in the cell periphery in *vps16a* RNAi cells (red arrows). **C:** In dynactin-kinesin-*vps16a* triple RNAi cells, autophagosomes are distributed throughout the cytoplasm. **D:** Overexpression of the recombinant minus-end motor Khc-nod-LacZ does not affect minus-end directed autophagosome transport in *vps16a* RNAi cells. **E:** Khc-nod-LacZ expression partially rescues the dynactin KD-induced peripheral redistribution of autophagosomes in *vps16a* RNAi cells. **F:** Quantification of data shown in A-E; n=10. Data for *dctn1-p150* RNAi is included as a positive control for peripheral distribution (shown in **Figure 2E**, K). The boundaries of RNAi or kinesin overexpressing cells are highlighted in magenta in the grayscale panels.

Rab7 and Rab39 and their effectors Epg5 and ema are required for bidirectional autophagosome transport

Rab small GTPases regulate vesicle transport and fusion by recruiting different effectors in their active, GTP-bound form (Stenmark, 2009). Therefore, we screened all the Rab small GTPases. In Rab7, or subunits of its guanine nucleotide exchange factor complex (Mon1-Ccz1) and its interactor Epg5 (Gillingham et al., 2014) knockdown Vps16A silencing cells, we could no longer observe the perinuclear accumulation of autophagosomes; they were scattered throughout the cytoplasm (**Fig. 4A-D, J**). Other hits were Rab39 and its interactor ema (Gillingham et al., 2014), both suggested to be involved in the regulation of lysosomal degradation (Kim et al., 2012; Kim et al., 2010; Lakatos et al., 2021; Zhang et al., 2023). Their phenotype was very similar (**Fig. 4E, F, J**, S3A, G) to Rab7 and Epg5.

Importantly, no other interaction partners of Rab7 and Rab39 appeared to be required for autophagosome transport (Supplementary File 1, Supplementary Table 1; examples shown in **Fig. 4G, H, J**), suggesting that mainly the Rab7-Epg5 and Rab39-ema interactions are required for the bidirectional motility of autophagosomes (**Fig. 4I**). Our results were also strengthened by immunolabelings of Atg8a and Rab7 (**Fig. 5A, B, E, F**, S3B-F, H, I). Importantly, autophagosomes were still dispersed in *epg5*, *vps16a* double RNAi cells, even if we overexpressed a YFP-Rab7 transgene, suggesting that Rab7 indeed regulates autophagosome positioning via Epg5 (**Fig. 5C, G**). Interestingly, Arl8 immunolabeling revealed that Epg5 loss does not influence the perinuclear positioning of non-fused lysosomes (**Fig. 5D, H**), suggesting that it exerts its function specifically on autophagosomes.

Therefore, we further analyzed Epg5 functions. We first generated an *epg5-9xHA* transgene driven by the *epg5* genomic promoter and expressed this reporter in *Drosophila* S2R+ cells. We found that this reporter colocalizes with both endogenous Rab7 and Atg8a (**Fig. 5I, J**). Epg5 has been suggested as a Rab7 effector both in fly (Gillingham et al., 2014) and in mammalian cells (Wang et al., 2016), which we could confirm as Epg5-9xHA coprecipitates with Rab7-FLAG in cultured fly cells (**Fig. 5K**). Moreover, Epg5-9xHA also coprecipitates with the endogenous dynein motor Dhc64C (**Fig. 5L**), supporting the idea that Rab7 via Epg5 is required for dynein-dependent autophagosome transport. Taking into consideration that Epg5 was found to regulate the positioning of autophagosomes but not lysosomes, we utilized garland nephrocytes to study its effect on endolysosome maturation. Nephrocytes maintain a constant rate of endocytosis, making them ideal tools to study the endolysosomal system (Lőrincz et al., 2016). We have previously shown that inhibited late endosome to lysosome maturation leads to the enlargement of the late endosomal compartment (Boda et al., 2019; Lőrincz et al., 2019; Lőrincz et al., 2016; Lőrincz, Tóth, et al., 2017). However, we found that neither the Rab7 or FYVE-GFP positive endosomal nor the Lamp1 positive lysosomal compartment changed upon the expression of *epg5* RNAi in nephrocytes (Fig. S4A-G). This was strengthened by ultrastructural analyses, which showed no obvious changes in the morphology of the endolysosomal compartment in *epg5* RNAi nephrocytes (Fig. S4H, I). These results suggest that in flies, Epg5 is an autophagosome-specific adaptor.

Knockdown of other small GTPases that play essential roles in the lysosomal system, such as Rab2 (Lőrincz, Tóth, et al., 2017), Rab5 (Poteryaev et al., 2010), Rab14 (Mauvezin et al., 2016), or Arl8 (Boda et al., 2019), did not change the perinuclear pattern of mCherry-Atg8a positive autophagosomes in *vps16a* RNAi cells (Fig. S5A-D, G). Notably, silencing the recycling endosomal Rab11 resulted in the scattering of mCherry-Atg8a puncta and the exceptionally strong accumulation of autophagosomes revealed by endogenous Atg8a staining (Fig. S5E-H). Rab11 has been shown to be involved in autophagosome maturation in flies (Szatmári et al., 2014), but neither Rab11 interactors resulted in any change in the perinuclear autophagosome distribution (Supplementary File 1, Supplementary Table 1), suggesting that the effects of Rab11 may be indirect, compared to our Rab7 and Rab39 hits.

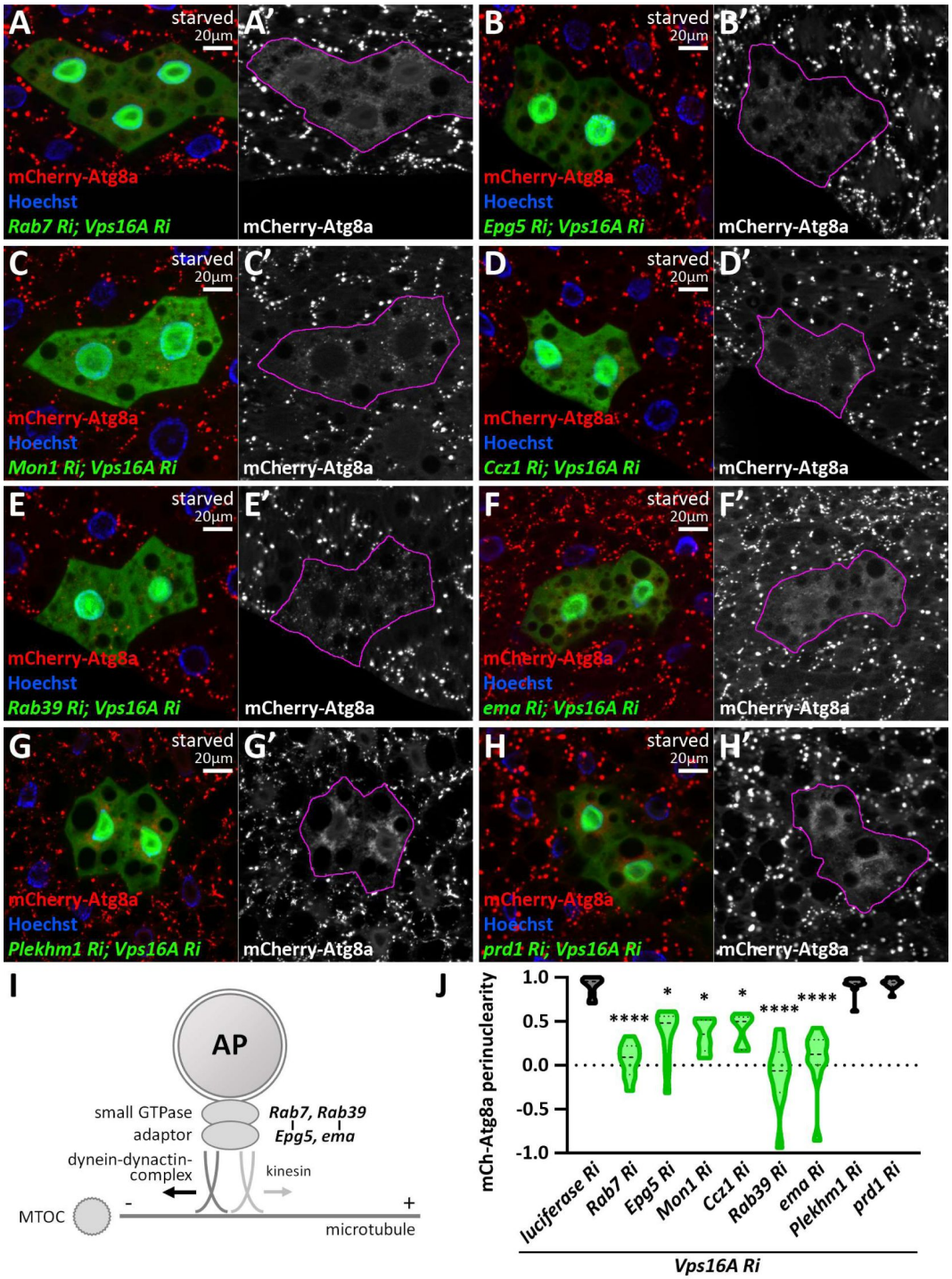

Figure 4.

Rab7 and Rab39 small GTPases and their interactors are responsible for bidirectional movement of autophagosomes.

A-H: Knockdown of Rab7 (A), its interactor Epg5 (B), the subunits of its guanine nucleotide exchange factor Mon1 (C) and Ccz1 (D), as well as Rab39 (E) and its interactor ema (F), inhibits the perinuclear positioning of autophagosomes in *vps16a* RNAi cells. In contrast, other factors such as Plekhm1 (G) and prd1 (H) do not affect autophagosome positioning. **I**: Proposed model of Rab small GTPases with their adaptors involved in autophagosome positioning. **J**: Quantification of data shown in A-H; n=10 cells. The boundaries of RNAi cells are highlighted in magenta in the grayscale panels.

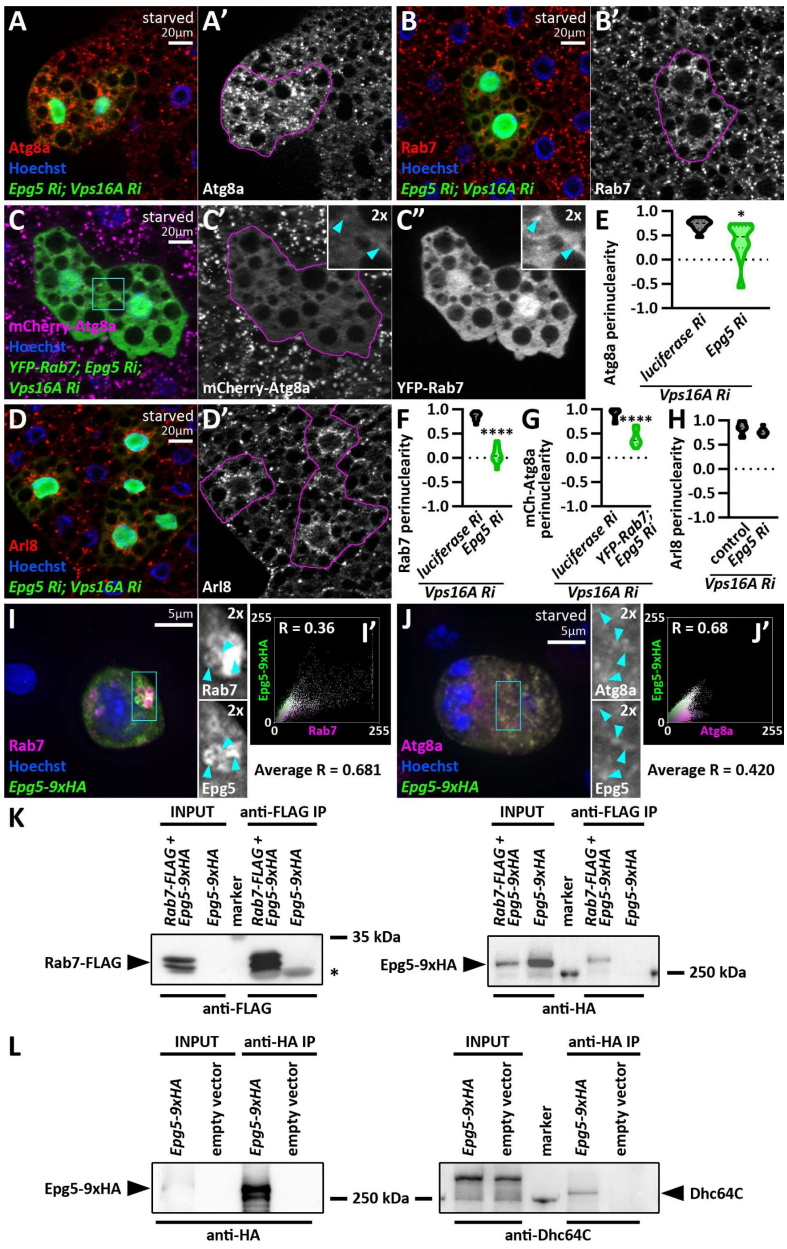

Figure 5.

Epg5 is responsible for bidirectional movement of autophagosomes.

A-B: The distribution of Atg8a (A) or Rab7 (B) positive autophagosomes becomes dispersed upon the expression of *epg5* and *vps16a* RNAi. **C:** Overexpression of YFP-tagged Rab7 does not rescue the scattered distribution of mCherry-Atg8a positive autophagosomes in the absence of Epg5 in *vps16a* RNAi cells, even though the colocalization of YFP-Rab7 with mCherry-Atg8a remains unaffected. Cyan arrowheads within insets (marked by a cyan box in panel C) point to YFP-Rab7 and mCherry-Atg8a double positive dots. **D:** The localization of Arl8 positive lysosomes remains perinuclear in *epg5*, *vps16a* double RNAi cells. The boundaries of RNAi and YFP-Rab7 expressing cells are highlighted in magenta in the grayscale panels. **E-H:** Quantification of data shown in A-D; n=10 cells. **I, J:** Epg5-9xHA colocalizes with endogenous Rab7 (I) or Atg8a (J) positive structures in S2R+ cells. Cyan arrowheads within insets (marked by cyan boxes in panels I and J) point to Epg5-9xHA and Rab7 or Atg8a double positive structures, respectively. I' and J' show scatter plots generated from the images of cells in panels I and J, respectively, depicting the intensity correlation profiles of Epg5-9xHA with Rab7 or Atg8a. Pearson correlation coefficients (R) are indicated, with the average R (n=10 cells) also shown, indicating colocalization in both cases. **K, L:** Coimmunoprecipitation experiments show that Epg5-9xHA binds to Rab7-FLAG (K) and endogenous Dhc64C (L) in cultured *Drosophila* cells. The asterisk in K marks immunoglobulin light chain.

Next, we analyzed the effect and localization of overexpressed autophagosomal and endolysosomal Rabs in *vps16a* RNAi cells. Neither the wild type nor the constitutively active forms of the overexpressed Rabs changed the perinuclear distribution of mCherry-Atg8a positive autophagosomes (Fig. S6A, B, D-L, N). Importantly, overexpression of both forms of YFP-tagged Rab7 (Fig. S6A, B) and Rab2 (Fig. S6D, E), as well as endogenous Rab7 immunolabeling (Fig. S6C) showed obvious autophagosomal localization. Moreover, wild type YFP-Rab39 also overlapped with the mCherry-Atg8a puncta (Fig. S6F) in *vps16a* RNAi cells. Our results suggest that Rab2 is exclusively required for autophagosomal fusions, while Rab7 and Rab39 are also required for autophagosome movement (Fig. S6M). The YFP-tagged wild type form of Rab14, which was described as a regulator of autophagic vesicle transport and fusion (Mauvezin et al., 2016), exhibited a punctate pattern, but did not localize to autophagosomes, suggesting that it localizes to other organelles, most likely lysosomes (Fig. S6L). Taken together, Rab7 and Rab39, as well as their effectors, Epg5 and ema, respectively, appear to be the most important regulators responsible for microtubular autophagosome motility in both directions.

The transport of pre-fusion lysosomes is also minus-end directed

Given that *vps16a* RNAi led to the perinuclear distribution of immature lysosomes (Fig. S1C) similar to autophagosomes, we hypothesized that pre-fusion autophagosomes and lysosomes travel in the same orientation, potentially sharing the same transport machinery. Thus, we stained lysosomes and co-expressed *vps16a* RNAi along with RNAi targeting our hits from the autophagosome positioning screen (Fig. S7). Importantly, in most cases, we observed similar phenotypes with Lamp1 staining as we did with Atg8a: spectraplakin (*shot*) RNAi redistributed Lamp1 organelles to an ectopic ncMTOC, dynein inhibition redistributed lysosomes to the periphery, *rab7*, *rab39*, and *ema* RNAi-s resulted in the scattering of lysosomes across the cytosol, and kinesin depletion had no effect on the perinuclear accumulation of lysosomes (Fig. S7).

However, there were two important exceptions: Epg5 knockdown left lysosomes perinuclear (Fig. S7C, L), suggesting that it is indeed an autophagosome-specific adaptor. The other exception was *rab2* RNAi, which had no significant effect on autophagosome transport but resulted in dispersed, and sometimes even peripheral, lysosomal distribution in Vps16A-depleted cells (Fig. S7I, L). This result suggests that Rab2 is a potential regulator of minus-end directed transport of lysosomes and that pre-fusion organelles (autophagosomes and lysosomes) predominantly travel towards the minus-end of the MTs and share the main molecular components.

Minus-end directed autophagosome and lysosome transport is required for autophagosome-lysosome fusion

We hypothesized that concentrating pre-fusion autophagosomes and lysosomes at the perinuclear region increases the probability of their fusion, thereby promoting autolysosome formation. To test this, we used similar reporters and reagents as above but did not silence Vps16A in the examined cells to allow autophagosome-lysosome fusions. First, we analyzed Epg5 knockdown, which has been described to inhibit autolysosome maturation based on GFP-Atg8a (Byrne et al., 2016) and we found it to be autophagosome-specific. In line with this, 3xmCherry-Atg8a positive autolysosomes were significantly smaller than in control cells, without any obvious change in their distribution (**Fig. 6A, B, E, F**). Accordingly, the large Rab7 and Arl8 positive autolysosomes were almost completely absent from Epg5 silenced cells, as revealed by immunostainings (**Fig. 6C, D, G, H**), with only small autolysosomes present.

In accordance with its suggested role in autophagosome-lysosome fusion, silencing of Rab7 resulted in significantly smaller and mostly dispersed autolysosomes (Fig. S8A, D, E) (Hegedűs et al., 2016; Lőrincz, Tóth, et al., 2017). Rab39 knockdown, however, led to mostly peripheral autolysosomes, which were not different in size from those in the control cells (Fig. S8B, D, E), but

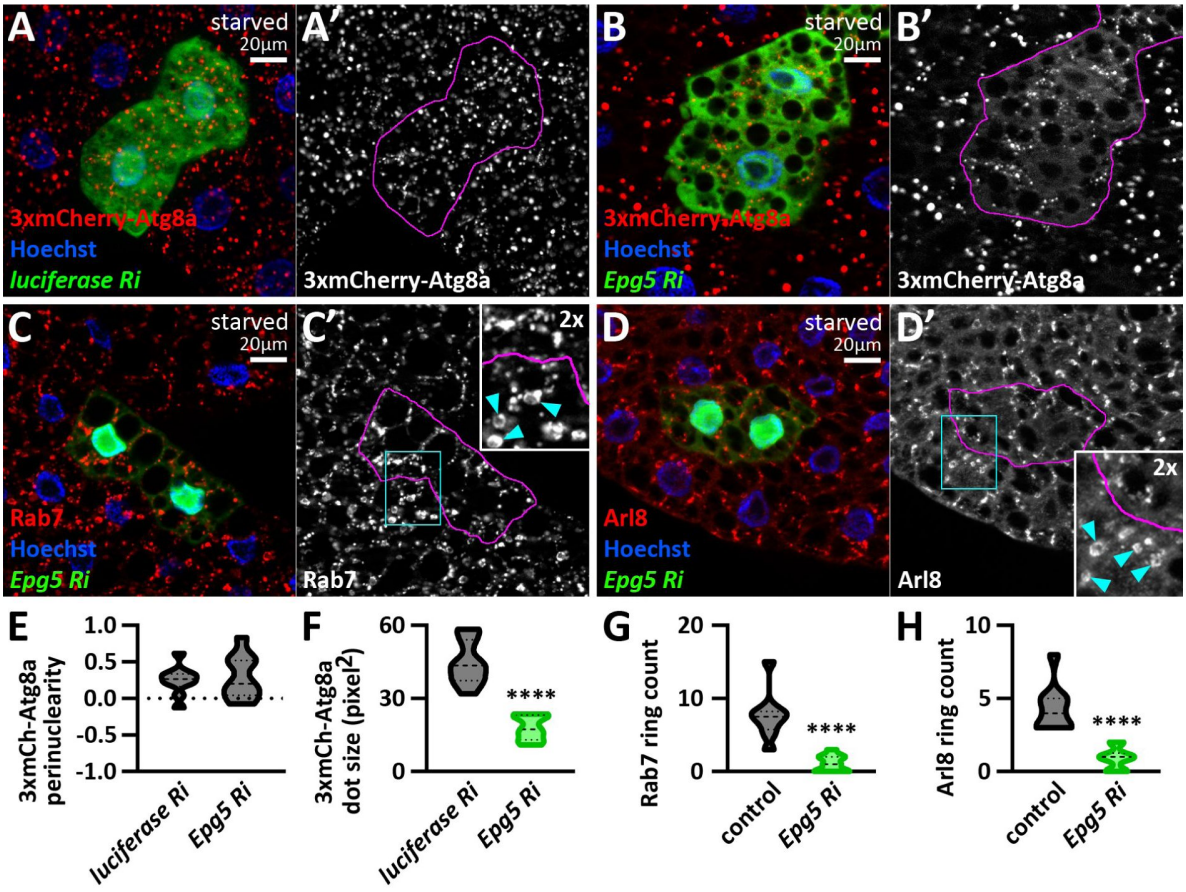

Figure 6.

Epg5 regulates autolysosome maturation.

A, B: Epg5 knockdown results in a significant reduction in the size of 3xmCherry-Atg8a positive autolysosomes (B) compared to control RNAi (*luciferase* RNAi) expressing cells (A). **C, D**: *Epg5* RNAi cells lack large Rab7 (C) and Arl8 (D) positive autolysosomes, which are present in surrounding control cells (cyan arrowheads in insets point to Rab7 and Arl8 positive autolysosomes in control cells). The boundaries of RNAi cells are highlighted in magenta in the grayscale panels. **E-H:** Quantification of data shown in A-D; n=10 cells.

the localization of the mCherry-Atg8a positive autolysosomes suggests that Rab39 is also required for minus-end directed movement of mature lysosomes. Surprisingly, loss of ema did not influence the size and distribution of autolysosomes (Fig. S8C-E).

Silencing of the dynein and dynactin hits: Dhc64C, sw, Dlic, and robl, as well as DCTN1-p150, resulted in the redistribution of 3xmCherry-Atg8a positive autolysosomes to the periphery and their size became significantly smaller (**Fig. 7A-E, I, K**), suggesting that loss of minus-end directed transport leads to autolysosome maturation defects. In contrast, *khc* and *klc* RNAi caused the perinuclear accumulation of autolysosomes, which appeared larger than those in the controls, suggesting a trend, although this difference did not reach statistical significance (**Fig. 7F, G, J, L**).

Our most important finding came when we silenced the spectraplakin Shot, which caused the accumulation of autolysosomes in the ectopic cytosolic MTOC (**Fig. 7H**). Notably, their size significantly increased (**Fig. 7H, L**). This can be explained by the fact that the volume surrounding the ectopic ncMTOC in Shot-depleted cells is smaller than the volume around the nuclei, leading to an increased fusion rate in these cells. Taken together, these results demonstrate that minus-end transport is crucial for proper autolysosome maturation.

The observation that dispersing autophagosomes and lysosomes under the plasma membrane in dynein/dynactin-silenced cells leads to insufficient autolysosome maturation, while concentrating autophagosomes and lysosomes to an ectopic ncMTOC in *shot* RNAi results in the enlargement of lysosomes, indicates that the autophagosome-lysosome fusion rate depends on the volume of cytoplasm in which these organelles meet. Several studies have suggested a connection between microtubular transport and the fusion of autophagosomes (Fass et al., 2006; Jahreiss et al., 2008; Kimura et al., 2008; Köchl et al., 2006).

We tested this hypothesis by analyzing the colocalization between the 3xmCherry-Atg8a reporter and the lysosomal membrane protein Lamp1, either by immunostaining or by expressing GFP-Lamp1. In control cells, Lamp1 or GFP-Lamp1 overlaps with mCherry-Atg8a, indicating that these organelles are indeed autolysosomes (**Fig. 8A, H, S9A, G**). In Shot-depleted cells, both signals overlapped in the ectopic ncMTOC, indicating that autophagosomes can effectively fuse with lysosomes in this region (**Fig. 8B, H, S9B, G**). Accordingly, the loss of the kinesin heavy chain Khc did not alter the overlap of these markers, proving that autolysosomes could still be formed (**Fig. 8C, H, S9C, G**). Importantly, the loss of the dynein motor Dhc64C, as well as the dynactin subunit DCTN1-p150, greatly reduced the overlap of signals, indicating a less effective autophagosome-lysosome fusion (**Fig. 8D, E, H**, S9D, G). Since Rab7 and Epg5 have been implicated in autolysosome maturation, their depletion reduced the overlap of autophagic and lysosomal markers (Byrne et al., 2016; Hegedűs et al., 2016; Wang et al., 2016) (**Fig. 8F-H**, S9E-G). Taken together, our results suggest that the purpose of minus-end directed transport in fat cells is to concentrate pre-fusion organelles to increase fusion probability.

Discussion

Microtubular transport of different organelles within the lysosomal system is essential for their proper function. Among the small GTPases that regulate late endosome/lysosome positioning, Rab7 (Fujiwara et al., 2016; Jordens et al., 2001; Ma et al., 2018; van der Kant et al., 2013) and Arl8 (Bagshaw et al., 2006; Boda et al., 2019; Hofmann & Munro, 2006; Marwaha et al., 2017; Rosa-Ferreira & Munro, 2011; Rosa-Ferreira et al., 2018) are well-studied. However, the positioning of autophagosomes is less understood. Autophagosome transport has been primarily studied in highly polarized neurons under basal conditions. In neuronal cells, dynein-mediated transport, regulated by several suggested adaptor molecules, has been described. However, most reporters and reagents used for studying autophagosome transport cannot differentiate between pre-fusion and post-fusion autophagic vesicles. Therefore, the regulation of

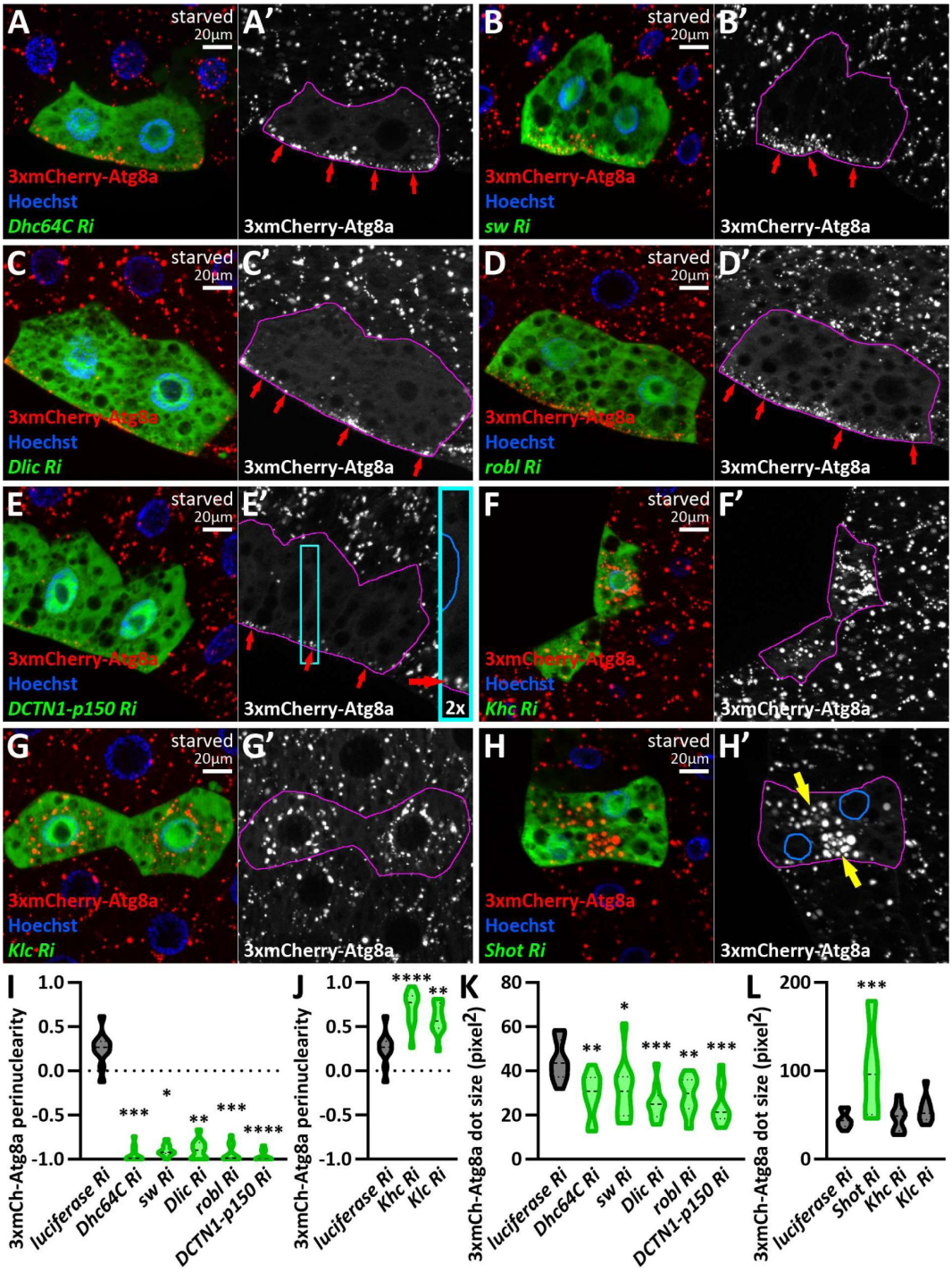

Figure 7.

Minus-end directed transport is required for autolysosome maturation.

A-E: Autolysosome size is significantly reduced upon the loss of dynein (A-D) or dynactin (E) function. Red arrows point to autolysosomes at the cell periphery in A'-E' and in the inset of E. **F, G:** Kinesin knockdowns do not significantly influence autolysosome size. **H:** Autolysosome size increases at ectopic foci (yellow arrows) in *shot* RNAi cells. The boundaries of RNAi-expressing cells are highlighted in magenta in the grayscale panels. The outlines of nuclei are drawn in blue in the inset of E' and in H'. **I-L:** Quantification of data shown in A-H; n=10 cells.

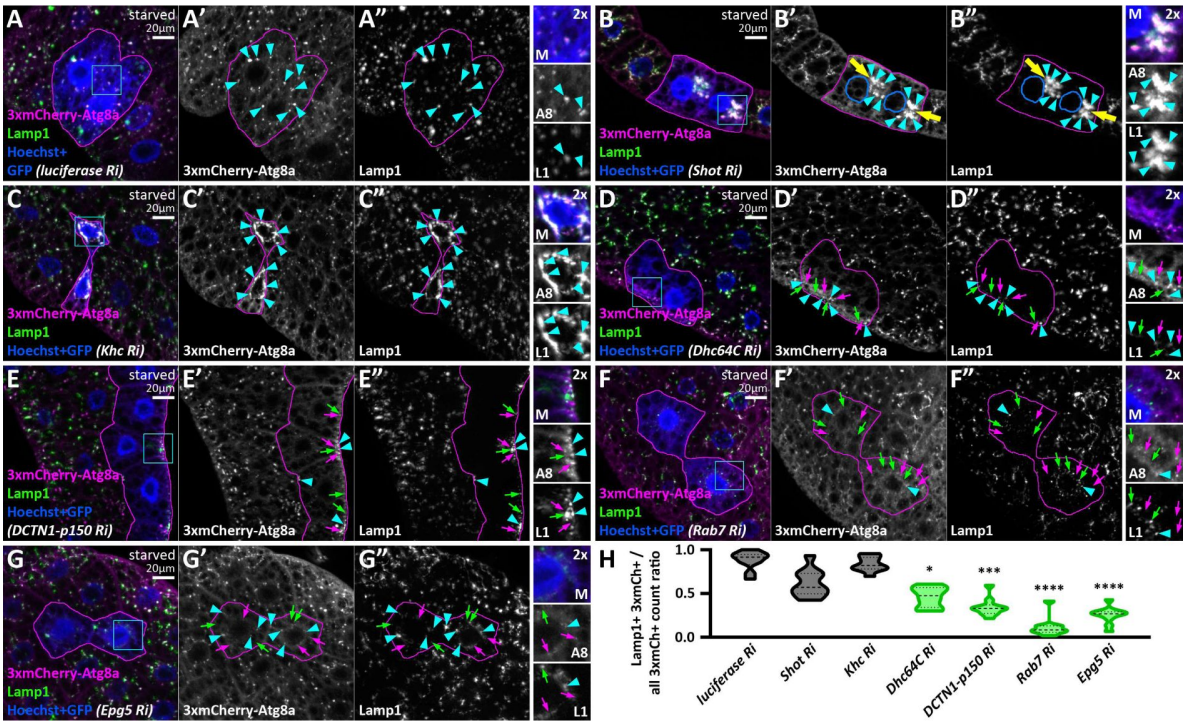

Figure 8.

Loss of the autophagosome positioning machinery decreases autophagosome-lysosome fusion.

A-G: In starved control RNAi (*luciferase*) expressing cells, mCherry-Atg8a overlaps with endogenous Lamp1 (A), indicating normal autophagosome-lysosome fusion and autolysosome formation. Autolysosomes still form in *shot* (B) or *khc* RNAi (C) cells, as mCherry-Atg8a colocalizes with endogenous Lamp1 similar to controls, but these are found in ectopic foci (yellow arrows) in *shot* RNAi cells. The outlines of nuclei are drawn in blue in B' and B''. Conversely, RNAi-s targeting factors responsible for minus-end directed autophagosome transport (D-G) decrease this overlap, suggesting less effective autophagosome-lysosome fusion. The GFP signal of RNAi-expressing cells is false-colored blue in composite images. The boundaries of RNAi-expressing cells are highlighted in magenta. Cyan arrowheads point to mCherry-Atg8a/Lamp1 double-positive structures, while magenta and green arrows indicate mCherry-Atg8a or Lamp1 single-positive dots, respectively. **H:** Quantification of data shown in A-G; n=10 cells.

non-fused autophagosome motility remains unclear. We propose that an autophagosome should not be considered as such once its lumen has started to acidify or undergo fusion, transitioning to a maturing autolysosome.

To address this issue, we established a genetic system generating mosaic cells where Vps16A, a central HOPS subunit, is silenced. Without Vps16A, cells are unable to fuse autophagosomes with lysosomes or late endosomes (Takáts et al., 2014), thus preventing the formation of autolysosomes. This system allowed us to study autophagosome positioning without misidentifying autolysosomes as autophagosomes. Given that fat cells have perinuclear non-centrosomal MTOCs, we hypothesized that non-fused autophagosomes move in a minus-end direction, likely driven by dyneins. This hypothesis was supported by our observation that relocating the ncMTOC using *shot* RNAi also relocated autophagosomes to this region.

Loss of dyneins and dynactins not only blocked perinuclear autophagosome positioning but also redistributed them to the cell periphery, suggesting that kinesin-regulated motility becomes available for starvation-induced autophagosomes in these conditions. Importantly, we showed that not all dyneins or dynactins are required for this transport. A dedicated cytosolic dynein complex, composed of Dhc64 (a heavy chain subunit), sw (an intermediate chain subunit), Dlic (a light intermediate chain subunit), and robl (a light chain subunit), activated by a dynactin complex, is required for autophagosome transport. This is consistent with observations that autophagosomes can move bidirectionally in neurons and that purified autophagosome fractions contain both dyneins and kinesins (Maday et al., 2012). Our results also reinforce findings that microtubule inhibitors block centrosome-directed autophagosome transport in mammalian cells (Fass et al., 2006).

Taking these observations into consideration, we investigated the relationship between dyneins and kinesins in autophagosome transport. Overexpression of kinesin motors blocked minus-end transport, while autophagosomes in kinesin and dynactin double knockdown cells appeared immobile. Moreover, expressing a recombinant minus-end kinesin (Clark et al., 1997) partially rescued the peripheral relocation of autophagosomes upon dynactin silencing, indicating a competitive relationship between minus- and plus-end motors in autophagosome positioning. The possibility of plus-end transport as a secondary mechanism raises questions about its physiological role. Besides enabling bidirectional movement (Jahreiss et al., 2008; Maday et al., 2012), it is possible that autophagosomes transport kinesins to autolysosomes, similar to endosomes, which are suggested to transport dyneins to autophagic vacuoles (Cheng et al., 2015). Therefore, if kinesins are present but are downregulated on autophagosomes, the absence of dyneins could potentially release them from inhibition. Autophagic vesicles are suggested to move towards the plus-end (Mauvezin et al., 2016; Pankiv et al., 2010), and loss of various kinesins leads to autophagosome accumulation in the cell center in mammalian cells (Cardoso et al., 2009; Korolchuk et al., 2011). The plus-end transport of autophagic vesicles by the Klp98A kinesin in *Drosophila* promotes autophagosome-lysosome fusion and degradation (Mauvezin et al., 2016). However, our tests indicated that Rab14 and its interactor Klp98A likely transport autolysosomes, not autophagosomes, as evidenced by the non-autophagosomal localization of YFP-Rab14 and that their RNAi-s had no effect on autophagosome positioning in starved, HOPS-depleted cells. Since neither kinesin RNAi altered the perinuclear accumulation of autophagosomes in Vps16A-depleted cells, we propose that the default direction is towards the MTOC at the minus-ends of microtubules.

Among Rab small GTPases, we identified Rab7 and Rab39 as regulators of autophagosome positioning. Rab7, crucial for autophagosome-lysosome fusion, appears on autophagosomes (Hegedűs et al., 2016). Its knockdown resulted in autophagosomes remaining randomly positioned in the cytosol, highlighting its importance in bidirectional motility. Consistent with our findings, Rab7 regulates both minus- and plus-end directed motility of lysosomes or endosomes, involving several adaptors such as Plekhm1 and FYCO1 (Fujiwara et al., 2016; Jordens et al.,

2001; Ma et al., 2018; Pankiv et al., 2010; Tabata et al., 2010; van der Kant et al., 2013). However, only one Rab7 interactor, the autophagy adaptor Epg5 (Gillingham et al., 2014; Wang et al., 2016), produced a similar phenotype to Rab7 in our tests. Additionally, we demonstrated that Epg5 coprecipitates with Dhc64C, and localizes to Rab7 and Atg8a-positive vesicles in cultured fruit fly cells. As Epg5 loss did not significantly impact the endolysosomal system, it appears to be autophagy-specific. Epg5 interacts with Rab7 and LC3 to mediate autophagosome-lysosome fusion in fly, worm and mammalian cells (Hori et al., 2017; Wang et al., 2016), and its mutations are linked to Vici syndrome, a severe neurodegenerative disorder in humans (Balasubramaniam et al., 2018; Byrne et al., 2016; Meneghetti et al., 2019). We thus identify a potential new role for Epg5 in autophagosome positioning.

Silencing Rab39 and its interactor ema (Gillingham et al., 2014) produced a phenotype similar to Rab7 or Epg5 loss. Rab39 regulates lysosomal function and interacts with HOPS in mammalian cells (Lakatos et al., 2021; Zhang et al., 2023). Ema promotes autophagosome biogenesis (Kim et al., 2012) and endosomal maturation through HOPS interaction (Kim et al., 2010). Our results suggest that Rab7-Epg5 and Rab39-ema interactions are both necessary for bidirectional autophagosome motility. Further studies are required to clarify their exact roles and interrelations. YFP-tagged Rab7 and Rab39 both colocalized with autophagosomes, supporting their role in motility. Rab2, Rab7, and Arl8 are known lysosomal fusion factors (Boda et al., 2019; Hegedűs et al., 2016; Lőrincz, Tóth, et al., 2017), but unlike Rab7, neither Rab2 nor Arl8 knockdown affected autophagosome positioning. Since YFP-Rab2 was also found to colocalize with autophagosomes, our results suggest that its sole role on autophagosomes is to regulate maturation.

Given the small Arl8-positive lysosomes in the perinuclear region upon Vps16A silencing, we hypothesized that pre-fusion lysosomes might exhibit similar motility to autophagosomes. This was largely confirmed, as minus-end transport of immature lysosomes depended on dyneins, Rab7, Rab39, and ema. However, Epg5 did not influence lysosome positioning, indicating its autophagosome-specific role. Conversely, Rab2 was identified as a regulator of minus-end directed lysosome transport. These findings suggest similar but distinct regulatory mechanisms for pre-fusion organelle transport, possibly to enhance fusion efficiency by converging them towards the cell center. Rab2's interaction with motor adaptors such as Bicaudal D (Gillingham et al., 2014) likely regulates lysosome motility.

Moreover, mature autolysosomes, but not pre-fusion ones, redistributed to the cell periphery upon Rab39 silencing, similar to dynein-depleted cells, suggesting that Rab39 exclusively regulates minus-end movement at the post-fusion level. Considering that plus-end directed lysosome motility is regulated by Arl8 (Bagshaw et al., 2006; Boda et al., 2019; Hofmann & Munro, 2006; Marwaha et al., 2017; Rosa-Ferreira & Munro, 2011; Rosa-Ferreira et al., 2018), which is dispensable for autophagosome motility, it is plausible that Rab39 promotes bidirectional transport of pre-fusion organelles, while its role post-fusion is restricted to minus-end directed motility.

An important question is why pre-fusion autophagosomes and lysosomes travel to the same destination. It is feasible to think this is because they need to fuse with each other. We found that loss of minus-end directed motility reduced autolysosome maturation; in dynein- or dynactin-depleted cells, only smaller autolysosomes were produced, and autophagosome-lysosome fusion decreased. This aligns with previous observations that dynein-regulated autophagosomal motility is indispensable for efficient lysosomal fusion (Jahreiss et al., 2008; Kimura et al., 2008). Conversely, inhibiting kinesins did not impede autophagosome-lysosome fusion, and concentrating autophagosomes and lysosomes to a smaller ectopic ncMTOC via *shot* RNAi resulted in enlarged lysosomes, allowing autophagosome-lysosome fusion to proceed.

Therefore, we propose a model in which pre-fusion organelles travel towards the MTOC in a cytosolic dynein-dependent manner regulated by small GTPases and their adaptors (Rab7-Epg5 and Rab39-ema on autophagosomes; Rab7, Rab39-ema, and Rab2 on lysosomes) to enhance fusion probability. After fusion, autolysosomes can move to the periphery in an Arl8-dependent manner and back, regulated by Rab39 (**Fig. 9**).

Materials and methods

Fly work and RNAi based screen

We raised the fly stocks and crosses in glass vials, on standard food at 25°C. Early third instar larvae were starved for 3 hours in 20% sucrose solution. Next fat bodies were dissected in cold PBS, mounted in a 8:2 mixture of glycerol and PBS completed with Hoechst 33342 as nuclear dye (5 µg/ml) (Thermo), then imaged immediately.

For the RNAi based genetic screen, we established the *hs-Flp; Vps16A RNAi, UAS-DCR2; act<CD2<Gal4, UAS-GFPnls, r4-mCherry-Atg8a* stock, in order to generate *vps16a* RNAi expressing fat cells. This was crossed with RNAi or overexpression lines of interest.

All the screened *Drosophila* lines, as well as their sources, identifiers and phenotypes are listed in Supplementary Table 1. Representative images of the phenotypes of screened lines are shown in Supplementary File 1. The proper genotypes and the fly stocks from the screen that were used in the Figure panels are summarized in Supplementary Table 2.

For further experiments, we used the following mosaic cell generating stocks, with or without Vps16A RNAi.:

- *- hs-Flp; Vps16A RNAi, UAS-DCR2; act<CD2<Gal4, UAS-GFPnls*,
- *- hs-Flp; UAS-DCR2; act<CD2<Gal4, UAS-GFPnls*,
- *- hs-Flp; 3xmCherry-Atg8a, UAS-2xEGFP; act<CD2<Gal4, UAS-DCR2*,
- *- hs-Flp; 3xmCherry-Atg8a, UAS-GFP-Lamp1; act<CD2<Gal4, UAS-DCR2*.

All of these stocks were described before (Boda et al., 2019; Lőrincz, Tóth, et al., 2017; Takáts et al., 2013). The *prospero-Gal4* driver (80572; FlyBase ID: FBst0080572) and the *UAS-GFP-myc-2xFYVE* reporter (42712; FlyBase ID: FBst0042712) used for the garland cell experiments were obtained from Bloomington Drosophila Stock Center.

Immunohistochemistry

For immunohistochemistry experiments, we dissected and fixed the samples in 4% paraformaldehyde (in PBS) for 45 min, washed them in PBS for 2×15 min, permeabilized in PBTX (0.1% Triton X-100 in PBS) for 20 min and blocked in 5% fetal bovine serum (in PBTX) for 30 min. The samples were then incubated with the primary antibodies (diluted in the blocking solution) overnight at 4°C, followed by washing in PBTX containing 4% NaCl for 15 min, washing in PBTX for 2×15 min, blocking in 5% fetal bovine serum (in PBTX) for 30 min and incubating with the secondary antibodies for 3 hours. The samples were then washed in PBTX containing 4% NaCl and 5 µg/ml Hoechst 33342 for 15 min, in PBTX for 2×15min, and in PBS for 2×15 min. All steps, except the incubation with primary antibodies, were performed at room temperature.

In case of garland immunohistochemistry and Lamp1 immunostainings of fat bodies for the 3xmCherry-Atg8a colocalization experiment, samples were dissected in a buffer containing 80 mM PIPES, 5 mM EGTA and 1 mM $MgCl_2$ (pH was adjusted to 6.8 with NaOH) and fixed in this solution containing also 3.7% formaldehyde, 0.25% glutaraldehyde and 0.2% Triton X-100, for 45 min.

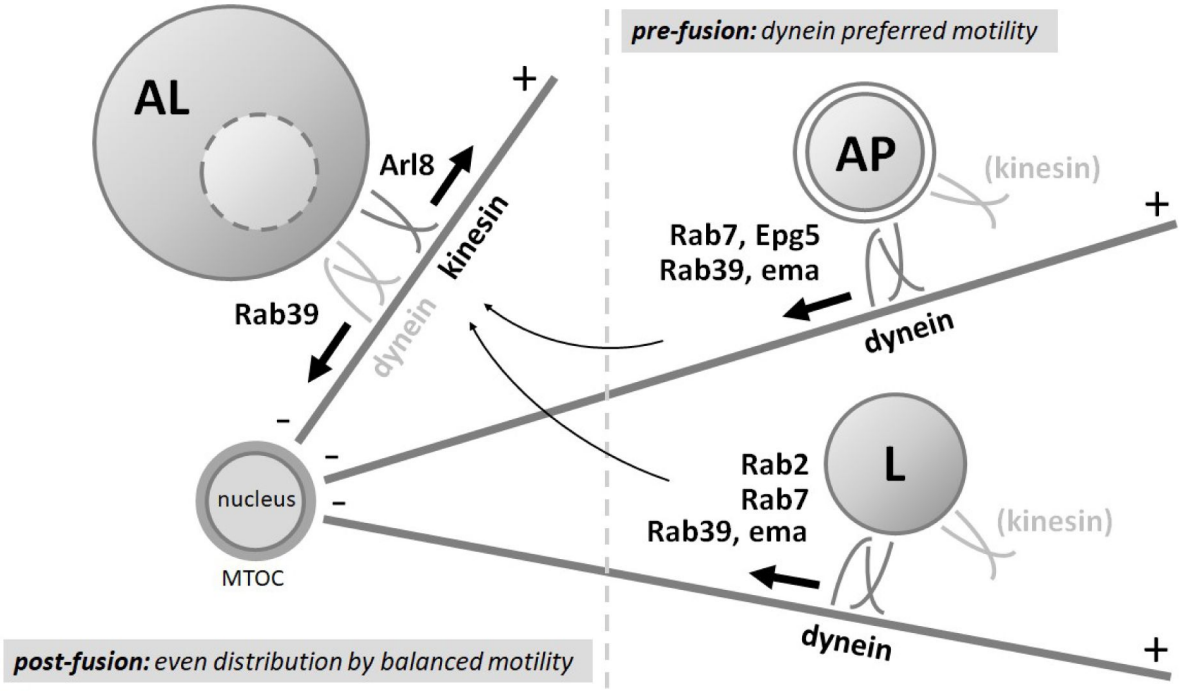

Figure 9.

Model of the transport of autophagosomes and lysosomes in starved fat cells.

Before fusion, autophagosomes and lysosomes are transported towards the perinuclear ncMTOC by a cytosolic dynein complex in starved fat cells to ensure proper fusion and effective degradation. This process requires Rab7, Rab39, and their interactors Epg5 and Ema on autophagosomes, and Rab2, Rab7, Rab39, and the Rab39 interactor Ema, but not Epg5, on lysosomes. After fusion, Arl8 mediates the plus- end transport of autolysosomes, while Rab39 promotes dynein-regulated minus-end directed transport. Thus, the motility of pre-fusion and post-fusion organelles is differently regulated: pre-fusion organelles generally move towards the MTOC, while post-fusion organelles exhibit bidirectional motility. This spatial regulation ensures proper fusion rates and degradation efficiency.

Following the fixation, the samples were incubated with 2 mg/ml sodium borohydride (in PBS) for 2.5 min, washed in PBS for 2×15 min (once for 10 min in case of garland cells) and permeabilized in PBTX containing ammonium chloride and glycine (both 50 mM) for 20 min. The remaining steps were the same as described above.

For immunostaining S2R+ hemocytes (*Drosophila*), cells were fixed in 4% paraformaldehyde for 20 min, washed in PBS for 15 min, permeabilized in PBTX for 10 min, and blocked in 5% fetal bovine serum (in PBTX) for 30 min. The samples were then incubated with the primary antibodies overnight at 4°C, followed by washing in PBTX containing 4% NaCl for 15 min and in PBTX for 2×10 min, and incubation with the secondary antibodies (solved in the blocking solution) for 3 h. The cells were then washed in PBTX containing 4% NaCl and 5 µg/ml Hoechst 33342 for 15 min, in PBTX for 10 min and in PBS for 15 min. In case of Atg8a immunolabeling, cells were starved in a solution containing 10 mM D(+) glucose, 0.5 mM $MgCl_2$, 4.5 mM KCl, 121 mM NaCl, 0.7 mM Na_2HPO_4, 1.5 mM NaH_2PO_4, and 15 mM $NaHCO_3$ (pH 7.4) (Aguilera-Gomez et al., 2017).

The following primary antibodies were used: rat anti-Atg8a (1:800; (Takáts et al., 2013)); rabbit anti-β-galactosidase (1:100; Merck); goat anti-Gmap (1:1000; Developmental Studies Hybridoma Bank [DSHB]); mouse anti-Rab7 (1:10; DSHB; (Riedel et al., 2016)); rabbit anti-Arl8 (1:300; DSHB); rabbit anti-Lamp1 (1:1000; (Chaudhry et al., 2022)), rat anti-mCherry (1:300; (Takáts et al., 2014); rabbit anti-HA (1:200; Merck) and chicken anti-GFP (1:1500; Invitrogen).

We used the following secondary antibodies: Alexa Fluor 568 goat anti-rat (1:1000); Alexa Fluor 647 donkey anti-rabbit (1:600); Alexa Fluor 568 donkey anti-goat (1:1000); Alexa Fluor 568 donkey anti-mouse (1:1000); Alexa Fluor 647 donkey-anti mouse (1:600); Alexa Fluor 568 donkey anti-rabbit (1:1000); Alexa Fluor 488 goat anti-chicken (1:1000) and Alexa Fluor 488 goat anti-rabbit (1:1000) (all Invitrogen).

Electron microscopy

For correlative ultrastructural analysis, fat bodies were dissected in a fixative containing 3.2% paraformaldehyde, 1% glutaraldehyde, 1% sucrose and 0.003 M $CaCl_2$ (in 0.1 N sodium cacodylate buffer, pH 7.4) on poly-L-lysine coated glass slides and fluorescent images were taken to help recognizing GFP and RNAi expressing cells. Then the samples were fixed in the same solution overnight at 4°C, then were post-fixed in 0.5% osmium tetroxide for 1 h, followed by half-saturated aqueous uranyl acetate for 30 min and dehydrated in a graded series of ethanol, followed by embedding into Durcupan ACM (Merck) on the glass slides. RNAi cells in the embedded samples were identified in semi-thick sections stained with toluidine blue, then ultra-thin sections of 70 nm were cut, then stained with Reynold's lead citrate (8 min, RT).

Preparation of samples for ultrastructural analysis of garland nephrocytes was performed as described before (Lőrincz et al., 2016).

Images were taken by a JEOL JEM-1011 transmission electron microscope operating at 80kV, equipped with a Morada camera (Olympus) and iTEM software (Olympus).

Molecular cloning and biochemistry Cloning

To generate *genEpg5-9xHA*, genomic DNA from *w1118 Drosophila* strain was isolated and used as a template. The genomic region containing *Drosophila CG14299* was amplified using primers 5'-CCAAGCTTGCATGCGGCCGCATTTTCTGTGCGCGACTGTTG-3' and 5'-TAAAAGATGCGGCCGGTACCGCCTCCACCCGTGGCCATTAACTTGAATTC-3' and cloned into *pGen-9xHA* (Lőrincz et al., 2016) as a NotI-Acc65I fragment by using Gibson Assembly kit (New England BioLabs, Ipswich, MA).

To obtain N-terminally 3xFLAG-tagged Rab7, the coding region of Rab7 was amplified from *Drosophila*cDNA using primers 5'-ACAAGGCGGCCGCAGGTATGTCCGGACGTAAGAAATCC-3' and 5'-TCTAGAGGTACCTTAGCACTGACAGTTGTCAGGA-3' and cloned into NotI-Acc65I sites of *pUAST-3xFLAG* vector (Takáts et al., 2014).

S2R+ maintenance and transfection

The S2R+ *Drosophila* cell line (Drosophila Genomics Resource Center; Stock 150; RRID: CVCL_Z831) was maintained in Insect XPress medium (Lonza) containing 10% FBS (EuroClone) and 1% Penicillin-Streptomycin (Lonza) at 26°C. Cells were transfected with *genEpg5-9xHA* plasmid using Calcium phosphate method. DNA was diluted in 240 mM $CaCl_2$, mixed with 2x HEPES-buffered saline (50 mM HEPES, 1.5 mM Na_2HPO_4, 280 mM NaCl, pH 7.1), incubated at 25°C for 30 minutes, and added to the cells. 24 hours after transfection, cells were used for immunohistochemistry or immunoprecipitation. In experiments, when cells were transfected with *pUAST-3xFLAG-Rab7* and *pGen-Epg5-9xHA* constructs, metallothionein-Gal4 plasmid was also applied. Protein expression was induced 24h after transfection with 500 µM $CuSO_4$ for overnight incubation.

Immunoprecipitation

Cells were transfected with appropriate plasmid constructs and were collected 24 hours after transfection. They were washed with PBS and lysed on ice in lysis buffer (0.5% Triton X-100, 150 mM NaCl, 5 mM EDTA, and 50 mM Tris-HCl, pH 7.5, complete protease inhibitor cocktail (Roche)) for 20 minutes. Cell lysates were cleared by centrifugation for 10 min at 20.000 g, 4°C, followed by the addition of mouse anti-HA or anti-FLAG agarose (Sigma-Aldrich) to the supernatant. After incubation at 4°C for 2 h, beads were collected by centrifugation at 5.000 g for 2 minutes at 4°C, followed by extensive washes in wash buffer (lysis buffer without protease inhibitors) and finally boiling in Laemmli sample buffer. Samples were analyzed by Western blot using rat anti-HA (1:1000; Roche), mouse anti-FLAG (M2; 1:2000; Sigma-Aldrich) and mouse anti-Dhc (2C11-2; 1:12.5; DSHB) antibodies. It is experimentally demonstrated that the Dhc antibody recognizes a polypeptide at around 260 kDa (Baker et al., 2021).

Imaging, quantification and statistics

We obtained the fluorescent images with an AxioImager M2 microscope (Zeiss), equipped with an ApoTome2 grid confocal unit (Zeiss) and with an Orca Flash 4.0 LT sCMOS camera (Hamamatsu), using Plan-Apochromat 40×/0.95 NA Air and Plan-Apochromat 63×/1.40 NA Oil objectives (Zeiss), and Zeiss Efficient Navigation 2 software. Images from eleven consecutive focal planes (section thickness: 0.35 µm in case of the 40× objective, and 0.25 µm in case of the 63× objective) were merged into one image. In case of S2R+ cells, fluorescent images were obtained with an Olympus IX83 inverted fluorescent microscope, equipped with an Orca FusionBT CMOS camera (Hamamatsu), using a Universal Plan Extended Apochromat 60×/1.42 NA objective (Olympus), and cellSens Dimension 4.1 software (Olympus). Images were taken with full optical sectioning of the cells; the focal planes were merged into one image and deconvolution was applied. Figures were produced in Photoshop CS5 Extended (Adobe).

Fluorescent structures were quantified either using ImageJ software (National Institutes of Health) or, in case of some types of experiment, manually. The signal threshold of the fluorescent channel of interest was set by the same person during quantifying one type of experiment with ImageJ. The fat cells, S2R+ cells and garland nephrocytes were randomly selected for quantification.

Structure distributions were quantified using ImageJ. In all cases, only cells with their nuclei in the focal plane were selected to ensure that both perinuclear and peripheral regions were included in quantifications. To quantify autophagosome distribution, we divided the fat cells into a perinuclear and a peripheral domain that were measured to be equal and calculated the area of the fluorescent signal in both domains. Then the difference of signal areas of the perinuclear and

peripheral domain was divided by the signal area of the entire cell, thus obtaining a ratio that represents the distribution of structures (1 – perfectly perinuclear, 0 – evenly dispersed, -1 – perfectly peripheral).

The counts of cells with ectopic ncMTOC (*shot* RNAi lines) and the Rab7/Arl8 ring counts (*epg5* RNAi) were determined manually by the same person, while the mCherry-Atg8a dot number (*atg8a* RNAi) and dot sizes were calculated using ImageJ. For quantifying Gmap signal intensity, mean gray values of neighboring control and RNAi cells were calculated by ImageJ. Colocalizations were quantified manually by the same person in case of fat body cells. Dot plots and Pearson's coefficients were calculated by ImageJ for evaluating colocalization in S2R+ cells.

To evaluate data from garland nephrocyte experiments, we used ImageJ to quantify fluorescent structures from unmodified single focal planes. To quantify the size of the Rab7 and FYVE-GFP positive endosomes, we measured the area of individual vesicles in the given focal plane of the cells. After setting the threshold for the fluorescent signal, we used the Watershed function of ImageJ coupled with manual segmentation when it was necessary to properly separate endosomes. For each genotype, we used 5 animals and measured the size of endosomes from a total of 10 cells. To quantify Lamp1 antibody staining signal in nephrocytes, we measured the area fraction of the cells covered by the given fluorescent signal at proper and uniform threshold settings. For each genotype, we used 5 late L3 stage animals and measured 15 cells.

Data were statistically evaluated using Prism 9.4.1 (GraphPad). The distribution of the datasets was determined using the D'Agostino & Pearson normality test. Parametric, unpaired, two-tailed t test or one-way ANOVA (with Dunnett multiple comparisons test) was used to compare two or more samples, respectively, all showing normal distribution. When comparing two or more samples that contained at least one variable showing non-Gaussian distribution, we used non-parametric Mann-Whitney test or Kruskal-Wallis test (with Dunn's multiple comparisons test), respectively. We showed the data as violin plots in the figures and represented p values as asterisks (<0.0001 ****; 0.0001-0.001 ***; 0.001-0.01 **; 0.01-0.05 *; 0.05< non-significant). Samples that are significantly different from the control are marked by green on the violin plots.

Acknowledgements

We thank Sarolta Pálfia for technical assistance, and colleagues and stock centers mentioned in the Materials and Methods section for supporting our work by providing fly stocks and reagents.

This work has been implemented with the support provided by the Ministry of Culture and Innovation of Hungary from the National Research, Development and Innovation Fund (PD142943 to AB; FK138851 to PL; KKP129797 to GJ; New National Excellence Program: ÚNKP-22-2-III-ELTE-702 and ÚNKP-23-3-I-ELTE-724 to DH, ÚNKP-23-3-I-ELTE-706 to MM), the Hungarian Academy of Sciences (LP2022-13/2022 to PL, LP-2014/2 to GJ) and the Eötvös Loránd University Excellence Fund (EKA 2022/045-P101-2 to PL).

The funders had no role in designing experiments, data collection and analysis, decision to publish, or preparation of the manuscript.

Additional information

Competing interests

The authors declare that no competing interests exist.

Author Contributions

AB, VB, and PL contributed to the study conception and experiment design. AB, PL, GJ, DH and MM acquired funding. Fly work, preparation of samples and fluorescent microscopy were performed by AB, VB, AN, DH, ML, FF and MM. Biochemistry experiments were performed by ZS. Ultrastructural analysis was performed by PL. Quantification and statistical analysis were performed by AB, VB and DH. The manuscript was written by AB and PL with comments from all authors.

References

Aguilera-Gomez A., Zacharogianni M., van Oorschot M. M., Genau H., Grond R., Veenendaal T., ..., Rabouille C. (2017) **Phospho-Rasputin Stabilization by Sec16 Is Required for Stress Granule Formation upon Amino Acid Starvation** *Cell Rep* **20**:935–948 https://doi.org/10.1016/j.celrep.2017.06.042

Bagshaw R. D., Callahan J. W., Mahuran D. J (2006) **The Arf-family protein, Arl8b, is involved in the spatial distribution of lysosomes** *Biochem Biophys Res Commun* **344**:1186–1191 https://doi.org/10.1016/j.bbrc.2006.03.221

Baker F. C., Neiswender H., Veeranan-Karmegam R., Gonsalvez G. B (2021) **In vivo proximity biotin ligation identifies the interactome of Egalitarian, a Dynein cargo adaptor** *Development* **148** https://doi.org/10.1242/dev.199935

Balasubramaniam S., Riley L. G., Vasudevan A., Cowley M. J., Gayevskiy V., Sue C. M., ..., Christodoulou J (2018) **EPG5-Related Vici Syndrome: A Primary Defect of Autophagic Regulation with an Emerging Phenotype Overlapping with Mitochondrial Disorders** *JIMD Rep* **42**:19–29 https://doi.org/10.1007/8904_2017_71

Boda A., Lőrincz P., Takáts S., Csizmadia T., Tóth S., Kovács A. L., Juhász G (2019) **Drosophila Arl8 is a general positive regulator of lysosomal fusion events** *Biochim Biophys Acta Mol Cell Res* **1866**:533–544 https://doi.org/10.1016/j.bbamcr.2018.12.011

Byrne S., Jansen L., U-King-Im J. M, Siddiqui A., Lidov H. G., Bodi I., ..., Jungbluth H (2016) **EPG5-related Vici syndrome: a paradigm of neurodevelopmental disorders with defective autophagy** *Brain* **139**:765–781 https://doi.org/10.1093/brain/awv393

Canty J. T., Tan R., Kusakci E., Fernandes J., Yildiz A (2021) **Structure and Mechanics of Dynein Motors** *Annu Rev Biophys* **50**:549–574 https://doi.org/10.1146/annurev-biophys-111020-101511

Cardoso C. M., Groth-Pedersen L., Høyer-Hansen M., Kirkegaard T., Corcelle E., Andersen J. S., ..., Nylandsted J (2009) **Depletion of kinesin 5B affects lysosomal distribution and stability and induces peri-nuclear accumulation of autophagosomes in cancer cells** *PLoS One* **4** https://doi.org/10.1371/journal.pone.0004424

Cason S. E., Carman P. J., Van Duyne C., Goldsmith J., Dominguez R., Holzbaur E. L. F. (2021) **Sequential dynein effectors regulate axonal autophagosome motility in a maturation-dependent pathway** *J Cell Biol* **220** https://doi.org/10.1083/jcb.202010179

Cason S. E., Holzbaur E. L. F (2023) **Axonal transport of autophagosomes is regulated by dynein activators JIP3/JIP4 and ARF/RAB GTPases** *J Cell Biol* **222** https://doi.org/10.1083/jcb.202301084

Chaudhry N., Sica M., Surabhi S., Hernandez D. S., Mesquita A., Selimovic A., ..., Jenny A (2022) **Lamp1 mediates lipid transport, but is dispensable for autophagy in Drosophila** *Autophagy* **18**:2443–2458 https://doi.org/10.1080/15548627.2022.2038999

Cheng X. T., Zhou B., Lin M. Y., Cai Q., Sheng Z. H (2015) **Axonal autophagosomes recruit dynein for retrograde transport through fusion with late endosomes** *J Cell Biol* **209**:377–386 https://doi.org/10.1083/jcb.201412046

Clark I. E., Jan L. Y., Jan Y. N (1997) **Reciprocal localization of Nod and kinesin fusion proteins indicates microtubule polarity in the Drosophila oocyte, epithelium, neuron and muscle** *Development* **124**:461–470 https://doi.org/10.1242/dev.124.2.461

Dix C. I., Soundararajan H. C., Dzhindzhev N. S., Begum F., Suter B., Ohkura H., ..., Bullock S. L (2013) **Lissencephaly-1 promotes the recruitment of dynein and dynactin to transported mRNAs** *J Cell Biol* **202**:479–494 https://doi.org/10.1083/jcb.201211052

Fass E., Shvets E., Degani I., Hirschberg K., Elazar Z (2006) **Microtubules support production of starvation-induced autophagosomes but not their targeting and fusion with lysosomes** *J Biol Chem* **281**:36303–36316 https://doi.org/10.1074/jbc.M607031200

Fu M. M., Nirschl J. J., Holzbaur E. L. F (2014) **LC3 binding to the scaffolding protein JIP1 regulates processive dynein-driven transport of autophagosomes** *Dev Cell* **29**:577–590 https://doi.org/10.1016/j.devcel.2014.04.015

Fujiwara T., Ye S., Castro-Gomes T., Winchell C. G., Andrews N. W., Voth D. E., ..., Zhao H (2016) **PLEKHM1/DEF8/RAB7 complex regulates lysosome positioning and bone homeostasis** *JCI Insight* **1** https://doi.org/10.1172/jci.insight.86330

Gillingham A. K., Sinka R., Torres I. L., Lilley K. S., Munro S (2014) **Toward a comprehensive map of the effectors of rab GTPases** *Dev Cell* **31**:358–373 https://doi.org/10.1016/j.devcel.2014.10.007

Hegedűs K., Takáts S., Boda A., Jipa A., Nagy P., Varga K., ..., Juhász G (2016) **The Ccz1-Mon1-Rab7 module and Rab5 control distinct steps of autophagy** *Mol Biol Cell* **27**:3132–3142 https://doi.org/10.1091/mbc.E16-03-0205

Hill S. E., Colón-Ramos D. A (2020) **The Journey of the Synaptic Autophagosome: A Cell Biological Perspective** *Neuron* **105**:961–973 https://doi.org/10.1016/j.neuron.2020.01.018

Hofmann I., Munro S (2006) **An N-terminally acetylated Arf-like GTPase is localised to lysosomes and affects their motility** *J Cell Sci* **119**:1494–1503 https://doi.org/10.1242/jcs.02958

Hori I., Otomo T., Nakashima M., Miya F., Negishi Y., Shiraishi H., ..., Saitoh S (2017) **Defects in autophagosome-lysosome fusion underlie Vici syndrome, a neurodevelopmental disorder with multisystem involvement** *Sci Rep* **7** https://doi.org/10.1038/s41598-017-02840-8

Ikenaka K., Kawai K., Katsuno M., Huang Z., Jiang Y. M., Iguchi Y., ..., Sobue G (2013) **dnc-1/dynactin 1 knockdown disrupts transport of autophagosomes and induces motor neuron degeneration** *PLoS One* **8** https://doi.org/10.1371/journal.pone.0054511

Jahreiss L., Menzies F. M., Rubinsztein D. C (2008) **The itinerary of autophagosomes: from peripheral formation to kiss-and-run fusion with lysosomes** *Traffic* **9**:574–587 https://doi.org/10.1111/j.1600-0854.2008.00701.x

Jordens I., Fernandez-Borja M., Marsman M., Dusseljee S., Janssen L., Calafat J., ..., Neefjes J (2001) **The Rab7 effector protein RILP controls lysosomal transport by inducing the recruitment of dynein-dynactin motors** *Curr Biol* **11**:1680–1685 https://doi.org/10.1016/s0960-9822(01)00531-0

Kim S., Naylor S. A., DiAntonio A (2012) **Drosophila Golgi membrane protein Ema promotes autophagosomal growth and function** *Proc Natl Acad Sci U S A* **109**:E1072–1081 https://doi.org/10.1073/pnas.1120320109

Kim S., Wairkar Y. P., Daniels R. W., DiAntonio A (2010) **The novel endosomal membrane protein Ema interacts with the class C Vps-HOPS complex to promote endosomal maturation** *J Cell Biol* **188**:717–734 https://doi.org/10.1083/jcb.200911126

Kimura S., Noda T., Yoshimori T (2008) **Dynein-dependent movement of autophagosomes mediates efficient encounters with lysosomes** *Cell Struct Funct* **33**:109–122 https://doi.org/10.1247/csf.08005

Korolchuk V. I., Saiki S., Lichtenberg M., Siddiqi F. H., Roberts E. A., Imarisio S., ..., Rubinsztein D. C (2011) **Lysosomal positioning coordinates cellular nutrient responses** *Nat Cell Biol* **13**:453–460 https://doi.org/10.1038/ncb2204

Köchl R., Hu X. W., Chan E. Y., Tooze S. A (2006) **Microtubules facilitate autophagosome formation and fusion of autophagosomes with endosomes** *Traffic* **7**:129–145 https://doi.org/10.1111/j.1600-0854.2005.00368.x

Lakatos Z., Benkő P., Juhász G., Lőrincz P (2021) **Drosophila Rab39 Attenuates Lysosomal Degradation** *Int J Mol Sci* **22** https://doi.org/10.3390/ijms221910635

Lee S., Sato Y., Nixon R. A (2011) **Lysosomal proteolysis inhibition selectively disrupts axonal transport of degradative organelles and causes an Alzheimer's-like axonal dystrophy** *J Neurosci* **31**:7817–7830 https://doi.org/10.1523/JNEUROSCI.6412-10.2011

Lei Y., Klionsky D. J (2021) **The Emerging Roles of Autophagy in Human Diseases** *Biomedicines* **9** https://doi.org/10.3390/biomedicines9111651

Lőrincz P., Juhász G (2020) **Autophagosome-Lysosome Fusion** *J Mol Biol* **432**:2462–2482 https://doi.org/10.1016/j.jmb.2019.10.028

Lőrincz P., Kenéz L. A., Tóth S., Kiss V., Varga Á., Csizmadia T., ..., Juhász G (2019) **Vps8 overexpression inhibits HOPS-dependent trafficking routes by outcompeting Vps41/Lt** *Elife* **8** https://doi.org/10.7554/eLife.45631

Lőrincz P., Lakatos Z., Varga Á., Maruzs T., Simon-Vecsei Z., Darula Z., ..., Juhász G (2016) **MiniCORVET is a Vps8-containing early endosomal tether in Drosophila** *Elife* **5** https://doi.org/10.7554/eLife.14226

Lőrincz P., Mauvezin C., Juhász G (2017) **Exploring Autophagy in Drosophila** *Cells* **6** https://doi.org/10.3390/cells6030022

Lőrincz P., Tóth S., Benkő P., Lakatos Z., Boda A., Glatz G., ..., Juhász G (2017) **Rab2 promotes autophagic and endocytic lysosomal degradation** *J Cell Biol* **216**:1937–1947 https://doi.org/10.1083/jcb.201611027

Ma X., Liu K., Li J., Li H., Liu Y., Yang C., Liang H (2018) **A non-canonical GTPase interaction enables ORP1L-Rab7-RILP complex formation and late endosome positioning** *J Biol Chem* **293**:14155–14164 https://doi.org/10.1074/jbc.RA118.001854

Maday S., Wallace K. E., Holzbaur E. L (2012) **Autophagosomes initiate distally and mature during transport toward the cell soma in primary neurons** *J Cell Biol* **196**:407–417 https://doi.org/10.1083/jcb.201106120

Marwaha R., Arya S. B., Jagga D., Kaur H., Tuli A., Sharma M (2017) **The Rab7 effector PLEKHM1 binds Arl8b to promote cargo traffic to lysosomes** *J Cell Biol* **216**:1051–1070 https://doi.org/10.1083/jcb.201607085

Mauvezin C., Neisch A. L., Ayala C. I., Kim J., Beltrame A., Braden C. R., ..., Neufeld T. P (2016) **Coordination of autophagosome-lysosome fusion and transport by a Klp98A-Rab14 complex in Drosophila** *J Cell Sci* **129**:971–982 https://doi.org/10.1242/jcs.175224

Meneghetti G., Skobo T., Chrisam M., Facchinello N., Fontana C. M., Bellesso S., ..., Dalla Valle L (2019) **The epg5 knockout zebrafish line: a model to study Vici syndrome** *Autophagy* **15**:1438–1454 https://doi.org/10.1080/15548627.2019.1586247

Neisch A. L., Neufeld T. P., Hays T. S (2017) **A STRIPAK complex mediates axonal transport of autophagosomes and dense core vesicles through PP2A regulation** *J Cell Biol* **216**:441–461 https://doi.org/10.1083/jcb.201606082

Olenick M. A., Holzbaur E. L. F (2019) **Dynein activators and adaptors at a glance** *J Cell Sci* **132** https://doi.org/10.1242/jcs.227132

Pankiv S., Alemu E. A., Brech A., Bruun J. A., Lamark T., Overvatn A., ..., Johansen T (2010) **FYCO1 is a Rab7 effector that binds to LC3 and PI3P to mediate microtubule plus end-directed vesicle transport** *J Cell Biol* **188**:253–269 https://doi.org/10.1083/jcb.200907015

Parzych K. R., Klionsky D. J (2014) **An overview of autophagy: morphology, mechanism, and regulation** *Antioxid Redox Signal* **20**:460–473 https://doi.org/10.1089/ars.2013.5371

Poteryaev D., Datta S., Ackema K., Zerial M., Spang A (2010) **Identification of the switch in early-to-late endosome transition** *Cell* **141**:497–508 https://doi.org/10.1016/j.cell.2010.03.011

Rahman A., Lőrincz P., Gohel R., Nagy A., Csordás G., Zhang Y., ..., Nezis I. P (2022) **GMAP is an Atg8a-interacting protein that regulates Golgi turnover in Drosophila** *Cell Rep* **39** https://doi.org/10.1016/j.celrep.2022.110903

Ravikumar B., Acevedo-Arozena A., Imarisio S., Berger Z., Vacher C., O'Kane C. J., ..., Rubinsztein D. C (2005) **Dynein mutations impair autophagic clearance of aggregate-prone proteins** *Nat Genet* **37**:771–776 https://doi.org/10.1038/ng1591

Redwine W. B., DeSantis M. E., Hollyer I., Htet Z. M., Tran P. T., Swanson S. K., ..., Reck-Peterson S. L (2017) **The human cytoplasmic dynein interactome reveals novel activators of motility** *Elife* **6** https://doi.org/10.7554/eLife.28257

Riedel F., Gillingham A. K., Rosa-Ferreira C., Galindo A., Munro S (2016) **An antibody toolkit for the study of membrane traffic in Drosophila melanogaster** *Biol Open* **5**:987–992 https://doi.org/10.1242/bio.018937

Rosa-Ferreira C., Munro S (2011) **Arl8 and SKIP act together to link lysosomes to kinesin-1** *Dev Cell* **21**:1171–1178 https://doi.org/10.1016/j.devcel.2011.10.007

Rosa-Ferreira C., Sweeney S. T., Munro S (2018) **The small G protein Arl8 contributes to lysosomal function and long-range axonal transport in** *Biol Open* **7** https://doi.org/10.1242/bio.035964

Scott R. C., Schuldiner O., Neufeld T. P (2004) **Role and regulation of starvation-induced autophagy in the Drosophila fat body** *Dev Cell* **7**:167–178 https://doi.org/10.1016/j.devcel.2004.07.009

Siller K. H., Serr M., Steward R., Hays T. S., Doe C. Q (2005) **Live imaging of Drosophila brain neuroblasts reveals a role for Lis1/dynactin in spindle assembly and mitotic checkpoint control** *Mol Biol Cell* **16**:5127–5140 https://doi.org/10.1091/mbc.e05-04-0338

Sitaram P., Anderson M. A., Jodoin J. N., Lee E., Lee L. A (2012) **Regulation of dynein localization and centrosome positioning by Lis-1 and asunder during Drosophila spermatogenesis** *Development* **139**:2945–2954 https://doi.org/10.1242/dev.077511

Stenmark H (2009) **Rab GTPases as coordinators of vesicle traffic** *Nat Rev Mol Cell Biol* **10**:513–525 https://doi.org/10.1038/nrm2728

Sun T., Song Y., Dai J., Mao D., Ma M., Ni J. Q., ..., Pastor-Pareja J. C (2019) **Spectraplakin Shot Maintains Perinuclear Microtubule Organization in Drosophila Polyploid Cells** *Dev Cell* **49**:731–747 https://doi.org/10.1016/j.devcel.2019.03.027

Swan A., Nguyen T., Suter B (1999) **Drosophila Lissencephaly-1 functions with Bic-D and dynein in oocyte determination and nuclear positioning** *Nat Cell Biol* **1**:444–449 https://doi.org/10.1038/15680

Szatmári Z., Kis V., Lippai M., Hegedus K., Faragó T., Lorincz P., ..., Sass M (2014) **Rab11 facilitates cross-talk between autophagy and endosomal pathway through regulation of Hook localization** *Mol Biol Cell* **25**:522–531 https://doi.org/10.1091/mbc.E13-10-0574

Tabata K., Matsunaga K., Sakane A., Sasaki T., Noda T., Yoshimori T (2010) **Rubicon and PLEKHM1 negatively regulate the endocytic/autophagic pathway via a novel Rab7-binding domain** *Mol Biol Cell* **21**:4162–4172 https://doi.org/10.1091/mbc.E10-06-0495

Takáts S., Nagy P., Varga Á., Pircs K., Kárpáti M., Varga K., ..., Juhász G (2013) **Autophagosomal Syntaxin17-dependent lysosomal degradation maintains neuronal function in Drosophila** *J Cell Biol* **201**:531–539 https://doi.org/10.1083/jcb.201211160

Takáts S., Pircs K., Nagy P., Varga Á., Kárpáti M., Hegedűs K., ..., Juhász G (2014) **Interaction of the HOPS complex with Syntaxin 17 mediates autophagosome clearance in Drosophila** *Mol Biol Cell* **25**:1338–1354 https://doi.org/10.1091/mbc.E13-08-0449

van der Kant R., Fish A., Janssen L., Janssen H., Krom S., Ho N., ..., Neefjes J. (2013) **Late endosomal transport and tethering are coupled processes controlled by RILP and the cholesterol sensor ORP1L** *J Cell Sci* **126**:3462–3474 https://doi.org/10.1242/jcs.129270

Vaughan K. T., Vallee R. B (1995) **Cytoplasmic dynein binds dynactin through a direct interaction between the intermediate chains and p150Glued** *J Cell Biol* :1507–1516 https://doi.org/10.1083/jcb.131.6.1507

Wang T., Martin S., Papadopulos A., Harper C. B., Mavlyutov T. A., Niranjan D., ..., Meunier F. A (2015) **Control of autophagosome axonal retrograde flux by presynaptic activity unveiled using botulinum neurotoxin type a** *J Neurosci* **35**:6179–6194 https://doi.org/10.1523/JNEUROSCI.3757-14.2015

Wang Z., Miao G., Xue X., Guo X., Yuan C., Zhang G., ..., Zhang H (2016) **The Vici Syndrome Protein EPG5 Is a Rab7 Effector that Determines the Fusion Specificity of Autophagosomes with Late Endosomes/Lysosomes** *Mol Cell* **63**:781–795 https://doi.org/10.1016/j.molcel.2016.08.021

Wong Y. C., Holzbaur E. L (2014) **The regulation of autophagosome dynamics by huntingtin and HAP1 is disrupted by expression of mutant huntingtin, leading to defective cargo degradation** *J Neurosci* **34**:1293–1305 https://doi.org/10.1523/JNEUROSCI.1870-13.2014

Zhang S., Tong M., Zheng D., Huang H., Li L., Ungermann C., ..., Zhong Q (2023) **C9orf72-catalyzed GTP loading of Rab39A enables HOPS-mediated membrane tethering and fusion in mammalian autophagy** *Nat Commun* **14** https://doi.org/10.1038/s41467-023-42003-0

Zheng Y., Buchwalter R. A., Zheng C., Wight E. M., Chen J. V., Megraw T. L (2020) **A perinuclear microtubule-organizing centre controls nuclear positioning and basement membrane secretion** *Nat Cell Biol* **22**:297–309 https://doi.org/10.1038/s41556-020-0470-7

Author information

Attila Boda
Department of Anatomy, Cell and Developmental Biology, Eötvös Loránd University, Budapest, Hungary, HAS-ELTE Momentum Vesicular Transport Research Group, Hungarian Academy of Sciences & ELTE Eötvös Loránd University, Budapest, Hungary
ORCID iD: 0000-0003-1811-8595

Villő Balázs
Department of Anatomy, Cell and Developmental Biology, Eötvös Loránd University, Budapest, Hungary, HAS-ELTE Momentum Vesicular Transport Research Group, Hungarian Academy of Sciences & ELTE Eötvös Loránd University, Budapest, Hungary

Anikó Nagy
Department of Anatomy, Cell and Developmental Biology, Eötvös Loránd University, Budapest, Hungary, HAS-ELTE Momentum Vesicular Transport Research Group, Hungarian Academy of Sciences & ELTE Eötvös Loránd University, Budapest, Hungary
ORCID iD: 0000-0002-0979-1617

Dávid Hargitai
Department of Anatomy, Cell and Developmental Biology, Eötvös Loránd University, Budapest, Hungary, HAS-ELTE Momentum Vesicular Transport Research Group, Hungarian Academy of Sciences & ELTE Eötvös Loránd University, Budapest, Hungary
ORCID iD: 0000-0002-6064-9966

Mónika Lippai
Department of Anatomy, Cell and Developmental Biology, Eötvös Loránd University, Budapest, Hungary, HAS-ELTE Momentum Vesicular Transport Research Group, Hungarian Academy of Sciences & ELTE Eötvös Loránd University, Budapest, Hungary
ORCID iD: 0000-0002-7307-4233

Zsófia Simon-Vecsei
Department of Anatomy, Cell and Developmental Biology, Eötvös Loránd University, Budapest, Hungary, HAS-ELTE Momentum Vesicular Transport Research Group, Hungarian Academy of Sciences & ELTE Eötvös Loránd University, Budapest, Hungary
ORCID iD: 0000-0001-7909-4895

Márton Molnár
Department of Anatomy, Cell and Developmental Biology, Eötvös Loránd University, Budapest, Hungary, HAS-ELTE Momentum Vesicular Transport Research Group, Hungarian Academy of Sciences & ELTE Eötvös Loránd University, Budapest, Hungary

Fanni Fürstenhoffer
Department of Anatomy, Cell and Developmental Biology, Eötvös Loránd University, Budapest, Hungary, HAS-ELTE Momentum Vesicular Transport Research Group, Hungarian Academy of Sciences & ELTE Eötvös Loránd University, Budapest, Hungary

Gábor Juhász
Department of Anatomy, Cell and Developmental Biology, Eötvös Loránd University, Budapest, Hungary, Lysosomal Degradation Research Group, Institute of Genetics, HUN-REN BRC Szeged, Szeged, Hungary
ORCID iD: 0000-0001-8548-8874

Péter Lőrincz
Department of Anatomy, Cell and Developmental Biology, Eötvös Loránd University, Budapest, Hungary, HAS-ELTE Momentum Vesicular Transport Research Group, Hungarian Academy of Sciences & ELTE Eötvös Loránd University, Budapest, Hungary
ORCID iD: 0000-0001-7374-667X

For correspondence: peter.lorincz@ttk.elte.hu

Editors

Reviewing Editor
Hitoshi Nakatogawa
Tokyo Institute of Technology, Yokohama, Japan

Senior Editor
Sofia Araújo
University of Barcelona, Barcelona, Spain

Reviewer #1 (Public review):

Summary:

It is well known that autophagosomes/autolysosomes move along microtubules. However, because previous studies did not distinguish between autophagosomes and autolysosomes, it

remains unknown whether autophagosomes begin to move after fusion with lysosomes or even before fusion. In this manuscript, the authors show, using fusion-deficient cells, that both pre-fusion autophagosomes and lysosomes can move along the MT toward the minus end. By screening motor proteins and Rabs, the authors found that autophagosomal traffic is primarily regulated by the dynein-dynactin system and can be counter-regulated by kinesins. They also show that Rab7-Epg5 and Rab39-ema interactions are important for autophagosome trafficking.

Strengths:

This study uses reliable Drosophila genetics and high-quality fluorescence microscopy. The data are properly quantified and statistically analyzed. It is a reasonable hypothesis that gathering pre-fusion autophagosomes and lysosomes in close proximity improves fusion efficiency.

Weaknesses:

(1) To distinguish autophagosomes from autolysosomes, the authors used vps16 RNAi cells, which are supposed to be fusion deficient. However, the extent to which fusion is actually inhibited by knockdown of Vps16A is not shown. The co-localization rate of Atg8 and Lamp1 should be shown (as in Figure 8). Then, after identifying pre-fusion autophagosomes and lysosomes, the localization of each should be analyzed. It is also possible that autophagosomes and lysosomes are tethered by factors other than HOPS (even if they are not fused). If this is the case, autophagosomal trafficking would be affected by the movement of lysosomes.

(2) The authors analyze autolysosomes in Figures 6 and 7. This is based on the assumption that autophagosome-lysosome fusion takes place in cells without vps16A RANi. However, even in the presence of Vps16A, both pre-fusion autophagosomes and autolysosomes should exist. This is also true in Figure 8H, where the fusion of autophagosomes and lysosomes is partially suppressed in knockdown cells of dynein, dynactin, Rab7, and Epg5. If the effect of fusion is to be examined, it is reasonable to distinguish between autophagosomes and autolysosomes and analyze only autolysosomes.

(3) In this study, only vps16a RNAi cells were used to inhibit autophagosome-lysosome fusion. However, since HOPS has many roles besides autophagosome-lysosome fusion, it would be better to confirm the conclusion by knockdown of other factors (e.g., Stx17 RNAi).

(4) Figure 8: Rab7 and Epg5 are also known to be directly involved in autophagosome-lysosome tethering/fusion. Even if the fusion rate is reduced in the absence of Rab7 and Epg5, it may not be the result of defective autophagosome movement, but may simply indicate that these molecules are required for fusion itself. How do the authors distinguish between the two possibilities?

https://doi.org/10.7554/eLife.102663.1.sa2

Reviewer #2 (Public review):

Summary:

This manuscript by Boda et al. describes the results of a targeted RNAi screen in the background of Vps16A-depleted Drosophila larval fat body cells. In this background, lysosomal fusion is inhibited, allowing the authors to analyze the motility and localization specifically of autophagosomes, prior to their fusion with lysosomes to become autolysosomes. In this Vps16A-deleted background, mCherry-Atg8a-labeled autophagosomes accumulate in the perinuclear area, through an unknown mechanism.

The authors found that the depletion of multiple subunits of the dynein/dynactin complex caused an alternation of this mCherry-Atg8a localization, moving from the perinuclear region to the cell periphery. Interactions with kinesin overexpression suggest these motor proteins may compete for autophagosome binding and transport. The authors extended these findings by examining potential upstream regulators including Rab proteins and selected effectors, and they also examined effects on lysosomal movement and autolysosome size. Altogether, the results are consistent with a model in which specific Rab/effector complexes direct the movement of lysosomes and autophagosomes toward the MTOC, promoting their fusion and subsequent dispersal throughout the cell.

Strengths:

Although previous studies of the movement of autophagic vesicles have identified roles for microtubule-based transport, this study moves the field forward by distinguishing between effects on pre- and post-fusion autophagosomes, and by its characterization of the roles of specific Dynein, Dynactin, and Rab complexes in regulating movement of distinct vesicle types. Overall, the experiments are well-controlled, appropriately analyzed, and largely support the authors' conclusions.

Weaknesses:

One limitation of the study is the genetic background that serves as the basis for the screening. In addition to preventing autophagosome-lysosome fusion, disruption of Vps16A has been shown to inhibit endosomal maturation and block the trafficking of components to the lysosome from both the endosome and Golgi apparatus. Additional effects previously reported by the authors include increased autophagosome production and reduced mTOR signaling. Thus Vps16A-depleted cells have a number of endosome, lysosome, and autophagosome-related defects, with unknown downstream consequences. Additionally, the cause and significance of the perinuclear localization of autophagosomes in this background is unclear. Thus, interpretations of the observed reversal of this phenotype are difficult, and have the caveat that they may apply only to this condition, rather than to normal autophagosomes. Additional experiments to observe autophagosome movement or positioning in a more normal environment would improve the manuscript.

Specific comments

(1) Several genes have been described that when depleted lead to perinuclear accumulation of Atg8-labeled vesicles. There seems to be a correlation of this phenotype with genes required for autophagosome-lysosome fusion; however, some genes required for lysosomal fusion such as Rab2 and Arl8 apparently did not affect autophagosome positioning as reported here. Thus, it is unclear whether the perinuclear positioning of autophagosomes is truly a general response to disruption of autophagosome-lysosome fusion, or may reflect additional aspects of Vps16A/HOPS function. A few things here would help. One would be an analysis of Atg8a vesicle localization in response to the depletion of a larger set of fusion-related genes. Another would be to repeat some of the key findings of this study (effects of specific dynein, dynactin, rabs, effectors) on Atg8a localization when Syx17 is depleted, rather than Vps16A. This should generate a more autophagosome-specific fusion defect. Third, it would greatly strengthen the findings to monitor pre-fusion autophagosome localization without disrupting fusion. Such vesicles could be identified as Atg8a-positive Lamp-negative structures. The effects of dynein and rab depletion on the tracking of these structures in a post-induction time course would serve as an important validation of the authors' findings.

(2) The authors nicely show that depletion of Shot leads to relocalization of Atg8a to ectopic foci in Vps16A-depleted cells; they should confirm that this is a mislocalized ncMTOC by co-labeling Atg8a with an MTOC component such as MSP300. The effect of Shot depletion on Atg8a localization should also be analyzed in the absence of Vps16A depletion.

(3) The authors report that depletion of Dynein subunits, either alone (Figure 6) or co-depleted with Vps16A (Figure 2), leads to redistribution of mCherry-Atg8a punctae to the "cell periphery". However, only cell clones that contact an edge of the fat body tissue are shown in these figures. Furthermore, in these cells, mCherry-Atg8a punctae appear to localize only to contact-free regions of these cells, and not to internal regions of clones that share a border with adjacent cells. Thus, these vesicles would seem to be redistributed to the periphery of the fat body itself, not to the periphery of individual cells. Microtubules emanating from the perinuclear ncMTOC have been described as having a radial organization, and thus it is unclear that this redistribution of mCherry-Atg8a punctae to the fat body edge would reflect a kinesin-dependent process as suggested by the authors.

(4) To validate whether the mCherry-Atg8a structures in Vps16A-depleted cells were of autophagic origin, the authors depleted Atg8a and observed a loss of mCherry- Atg8a signal from the mosaic cells (Figure S1D, J). A more rigorous experiment would be to deplete other Atg genes (not Atg8a) and examine whether these structures persist.

(5) The authors found that only a subset of dynein, dynactin, rab, and rab effector depletions affected mCherry- Atg8a localization, leading to their suggestion that the most important factors involved in autophagosome motility have been identified here. However, this conclusion has the caveat that depletion efficiency was not examined in this study, and thus any conclusions about negative results should be more conservative.

https://doi.org/10.7554/eLife.102663.1.sa1

Reviewer #3 (Public review):

Summary:

In multicellular organisms, autophagosomes are formed throughout the cytosol, while late endosomes/lysosomes are relatively confined in the perinuclear region. It is known that autophagosomes gain access to the lysosome-enriched region by microtubule-based trafficking. The mechanism by which autophagosomes move along microtubules remains incompletely understood. In this manuscript, Péter Lőrincz and colleagues investigated the mechanism driving the movement of nascent autophagosomes along the microtubule towards the non-centrosomal microtubule organizing center (ncMTOC) using the fly fat body as a model system. The authors took an approach whereby they examined autophagosome positioning in cells where autophagosome-lysosome fusion was inhibited by knocking down the HOPS subunit Vps16A. Despite being generated at random positions in the cytosol, autophagosomes accumulate around the nucleus when Vps16A is depleted. They then performed an RNA interference screen to identify the factors involved in autophagosome positioning. They found that the dynein-dynactin complex is required for the trafficking of autophagosomes toward ncMTOC. Dynein loss leads to the peripheral relocation of autophagosomes. They further revealed that a pair of small GTPases and their effectors, Rab7-Epg5 and Rab39-ema, are required for bidirectional autophagosome transport. Knockdown of these factors in Vps16a RNAi cells causes the scattering of autophagosomes throughout the cytosol.

Strengths:

The data presented in this study help us to understand the mechanism underlying the trafficking and positioning of autophagosomes.

Weaknesses:

Major concerns:

(1) The localization of EPG5 should be determined. The authors showed that EPG5 colocalizes with endogenous Rab7. Rab7 labels late endosomes and lysosomes. Previous studies in mammalian cells have shown that EPG5 is targeted to late endosomes/lysosomes by interacting with Rab7. EPG5 promotes the fusion of autophagosomes with late endosomes/lysosomes by directly recognizing LC3 on autophagosomes and also by facilitating the assembly of the SNARE complex for fusion. In Figure 5I, the EPG5/Rab7-colocalized vesicles are large and they are likely to be lysosomes/autolysosomes.

(2) The experiments were performed in Vps16A RNAi KD cells. Vps16A knockdown blocks fusion of vesicles derived from the endolysosomal compartments such as fusion between lysosomes. The pleiotropic effect of Vps16A RNAi may complicate the interpretation. The authors need to verify their findings in Stx17 KO cells, as it has a relatively specific effect on the fusion of autophagosomes with late endosomes/lysosomes.

(3) Quantification should be performed in many places such as in Figure S4D for the number of FYVE-GFP labeled endosomes and in Figures S4H and S4I for the number and size of lysosomes.

(4) In this study, the transport of autophagosomes is investigated in fly fat cells. In fat cells, a large number of large lipid droplets accumulate and the endomembrane systems are distinct from that in other cell types. The knowledge gained from this study may not apply to other cell types. This needs to be discussed.

Minor concerns:

(5) Data in some panels are of low quality. For example, the mCherry-Atg8a signal in Figure 5C is hard to see; the input bands of Dhc64c in Figure 5L are smeared.

(6) In this study, both 3xmCherry-Atg8a and mCherry-Atg8a were used. Different reporters make it difficult to compare the results presented in different figures.

(7) The small autophagosomes presented in Figures such as in Figure 1D and 1E are not clear. Enlarged images should be presented.

(8) The authors showed that Epg5-9xHA coprecipitates with the endogenous dynein motor Dhc64C. Is Rab7 required for the interaction?

(9) The perinuclear lysosome localization in Epg5 KD cells has no indication that Epg5 is an autophagosome-specific adaptor.

https://doi.org/10.7554/eLife.102663.1.sa0

Author Response:

> ***Reviewer #1 (Public review):***
>
> *Summary:*
>
> *It is well known that autophagosomes/autolysosomes move along microtubules. However, because previous studies did not distinguish between autophagosomes and autolysosomes, it remains unknown whether autophagosomes begin to move after fusion with lysosomes or even before fusion. In this manuscript, the authors show, using fusion-deficient cells, that both pre-fusion autophagosomes and lysosomes can move along the MT toward the minus end. By screening motor proteins and Rabs, the authors found that autophagosomal traffic is primarily regulated by the dynein-dynactin system*

> *and can be counter-regulated by kinesins. They also show that Rab7-Epg5 and Rab39-ema interactions are important for autophagosome trafficking.*
>
> *Strengths:*
>
> *This study uses reliable Drosophila genetics and high-quality fluorescence microscopy. The data are properly quantified and statistically analyzed. It is a reasonable hypothesis that gathering pre-fusion autophagosomes and lysosomes in close proximity improves fusion efficiency.*

Thank you for your positive comments and for acknowledging the strengths of our work.

> *Weaknesses:*
>
> *(1) To distinguish autophagosomes from autolysosomes, the authors used vps16 RNAi cells, which are supposed to be fusion deficient. However, the extent to which fusion is actually inhibited by knockdown of Vps16A is not shown. The co-localization rate of Atg8 and Lamp1 should be shown (as in Figure 8). Then, after identifying pre-fusion autophagosomes and lysosomes, the localization of each should be analyzed.*

Thank you for this comment. We plan to perform immunohistochemistry experiment on Vps16A KD fat body cells for mCherry and Lamp1, as in case of other panels of Figure 8. We will also analyse the distribution of each.

> *It is also possible that autophagosomes and lysosomes are tethered by factors other than HOPS (even if they are not fused). If this is the case, autophagosomal trafficking would be affected by the movement of lysosomes.*

While we cannot exclude the possibility that autophagosomes are transported indirectly by being tethered to lysosomes. However, we find this unlikely be the case as we believe in fat cells lysosomes and autophagosomes will rapidly fuse with each other if they get close enough.

> *(2) The authors analyze autolysosomes in Figures 6 and 7. This is based on the assumption that autophagosome-lysosome fusion takes place in cells without vps16A RANi. However, even in the presence of Vps16A, both pre-fusion autophagosomes and autolysosomes should exist. This is also true in Figure 8H, where the fusion of autophagosomes and lysosomes is partially suppressed in knockdown cells of dynein, dynactin, Rab7, and Epg5. If the effect of fusion is to be examined, it is reasonable to distinguish between autophagosomes and autolysosomes and analyze only autolysosomes.*

Thank you for your careful insights. The mCherry-Atg8a reporter we use is highly stable in autolysosomes due to the resilience of the mCherry fluorophore within these acidic, post-fusion structures, making it useful for labelling both autophagosomes and autolysosomes. Notably, the high intensity of mCherry-Atg8a within autolysosomes allows us to distinguish them from pre-fusion autophagosomes, which appear fainter and smaller, especially when accumulated in fusion-defective backgrounds (as shown in Figure 4). We therefore regard larger, brighter structures as autolysosomes.

To improve clarity, we included additional markers—endogenous Lamp1 staining (Figure 8) and Lamp1-GFP (Figure S9)—to help differentiate between autophagic structures. Lamp1-negative, mCherry-Atg8a-positive vesicles indicate pre-fusion autophagosomes, while Lamp1/mCherry-Atg8a double-positive vesicles represent autolysosomes. Additionally,

Lamp1-positive, mCherry-Atg8a-negative vesicles mark lysosomes of non-autophagic origin. We appreciate your suggestion

> *(3) In this study, only vps16a RNAi cells were used to inhibit autophagosome-lysosome fusion. However, since HOPS has many roles besides autophagosome-lysosome fusion, it would be better to confirm the conclusion by knockdown of other factors (e.g., Stx17 RNAi).*

Thank you for this suggestion. We will generate additional Drosophila lines similar to those used in our current study, substituting Syntaxin17, SNAP29 or Vamp7 RNAi for Vps16A RNAi. We will test key phenotypic hits with these new backgrounds to confirm our findings.

> *(4) Figure 8: Rab7 and Epg5 are also known to be directly involved in autophagosome-lysosome tethering/fusion. Even if the fusion rate is reduced in the absence of Rab7 and Epg5, it may not be the result of defective autophagosome movement, but may simply indicate that these molecules are required for fusion itself. How do the authors distinguish between the two possibilities?*

Thank you for this comment. While we agree that Rab7 and Epg5 are involved in autophagosome-lysosome tethering and subsequent fusion, we believe they also play an additional role in autophagosome movement. Our hypothesis stems from the observation that the phenotypes of vps16 RNAi and rab7 or epg5 RNAi are not identical. In contrast, RNAi targeting SNARE proteins involved exclusively in fusion (Syx17, SNAP29, and Vamp7) all result in a consistent phenotype: autophagosomes accumulate around the nucleus, closely resembling the phenotype observed with vps16 depletion. This suggests that these SNAREs are specifically involved in fusion. Since Rab7 and Epg5 depletion scatters autophagosomes throughout the cytosol rather than transporting them to the nucleus, we hypothesize that this is due to impaired movement of autophagosomes. This hypothesis is further supported by our co-IP data showing that Epg5 binds to dyneins.

> ***Reviewer #2 (Public review):***
>
> *Summary:*
>
> *This manuscript by Boda et al. describes the results of a targeted RNAi screen in the background of Vps16A-depleted Drosophila larval fat body cells. In this background, lysosomal fusion is inhibited, allowing the authors to analyze the motility and localization specifically of autophagosomes, prior to their fusion with lysosomes to become autolysosomes. In this Vps16A-deleted background, mCherry-Atg8a-labeled autophagosomes accumulate in the perinuclear area, through an unknown mechanism.*
>
> *The authors found that the depletion of multiple subunits of the dynein/dynactin complex caused an alternation of this mCherry-Atg8a localization, moving from the perinuclear region to the cell periphery. Interactions with kinesin overexpression suggest these motor proteins may compete for autophagosome binding and transport. The authors extended these findings by examining potential upstream regulators including Rab proteins and selected effectors, and they also examined effects on lysosomal movement and autolysosome size. Altogether, the results are consistent with a model in which specific Rab/effector complexes direct the movement of lysosomes and autophagosomes toward the MTOC, promoting their fusion and subsequent dispersal throughout the cell.*
>
> *Strengths:*
>
> *Although previous studies of the movement of autophagic vesicles have identified roles for microtubule-based transport, this study moves the field forward by distinguishing between effects on pre- and post-fusion autophagosomes, and by its characterization of*

> *the roles of specific Dynein, Dynactin, and Rab complexes in regulating movement of distinct vesicle types. Overall, the experiments are well-controlled, appropriately analyzed, and largely support the authors' conclusions.*

Thank you for your positive comments and for acknowledging the strengths of our work.

> *Weaknesses:*
>
> *One limitation of the study is the genetic background that serves as the basis for the screening. In addition to preventing autophagosome-lysosome fusion, disruption of Vps16A has been shown to inhibit endosomal maturation and block the trafficking of components to the lysosome from both the endosome and Golgi apparatus. Additional effects previously reported by the authors include increased autophagosome production and reduced mTOR signaling. Thus Vps16A-depleted cells have a number of endosome, lysosome, and autophagosome-related defects, with unknown downstream consequences. Additionally, the cause and significance of the perinuclear localization of autophagosomes in this background is unclear. Thus, interpretations of the observed reversal of this phenotype are difficult, and have the caveat that they may apply only to this condition, rather than to normal autophagosomes. Additional experiments to observe autophagosome movement or positioning in a more normal environment would improve the manuscript.*

Thank you for highlighting this limitation. We plan to conduct time-lapse imaging of live fat body tissues expressing 3xmCherry-Atg8a and GFP-Lamp1 to visualize the movement and fusion events of pre-fusion autophagosomes (3xmCherry-Atg8a positive and GFP-Lamp1 negative) and lysosomes (GFP-Lamp1 positive). We expect these vesicles to exhibit movement toward the ncMTOC, providing insight into their behaviour under more typical conditions.

> *Specific comments*
>
> *(1) Several genes have been described that when depleted lead to perinuclear accumulation of Atg8-labeled vesicles. There seems to be a correlation of this phenotype with genes required for autophagosome-lysosome fusion; however, some genes required for lysosomal fusion such as Rab2 and Arl8 apparently did not affect autophagosome positioning as reported here. Thus, it is unclear whether the perinuclear positioning of autophagosomes is truly a general response to disruption of autophagosome-lysosome fusion, or may reflect additional aspects of Vps16A/HOPS function. A few things here would help. One would be an analysis of Atg8a vesicle localization in response to the depletion of a larger set of fusion-related genes. Another would be to repeat some of the key findings of this study (effects of specific dynein, dynactin, rabs, effectors) on Atg8a localization when Syx17 is depleted, rather than Vps16A. This should generate a more autophagosome-specific fusion defect.*

Thank you for this suggestion. We will generate additional Drosophila lines similar to those used in our current study, substituting Syntaxin17, SNAP29, and Vamp7 RNAi for Vps16A RNAi. We will test key phenotypic hits with these new backgrounds to confirm our findings.

> *Third, it would greatly strengthen the findings to monitor pre-fusion autophagosome localization without disrupting fusion. Such vesicles could be identified as Atg8a-positive Lamp-negative structures. The effects of dynein and rab depletion on the tracking of these structures in a post-induction time course would serve as an important validation of the authors' findings.*

Thank you for this helpful suggestion. We plan to conduct time-lapse experiments under various conditions (e.g., non-starved and starved at different durations) to monitor the

motility of newly formed autophagosomes (3xmCherry-Atg8a positive, Lamp1 negative), allowing us to analyze their positioning dynamics without interference from fusion defects.

> *(2) The authors nicely show that depletion of Shot leads to relocalization of Atg8a to ectopic foci in Vps16A-depleted cells; they should confirm that this is a mislocalized ncMTOC by co-labeling Atg8a with an MTOC component such as MSP300. The effect of Shot depletion on Atg8a localization should also be analyzed in the absence of Vps16A depletion.*

Thank you for this positive comment, to confirm the presence of ectopic MTOC foci in Shot KD cells, we plan to co-label with MTOC markers, including Khc-nod-LacZ, and additional reporters like Msps-mCherry, in both Vps16A-depleted and normal backgrounds.

> *(3) The authors report that depletion of Dynein subunits, either alone (Figure 6) or co-depleted with Vps16A (Figure 2), leads to redistribution of mCherry-Atg8a punctae to the "cell periphery". However, only cell clones that contact an edge of the fat body tissue are shown in these figures. Furthermore, in these cells, mCherry-Atg8a punctae appear to localize only to contact-free regions of these cells, and not to internal regions of clones that share a border with adjacent cells. Thus, these vesicles would seem to be redistributed to the periphery of the fat body itself, not to the periphery of individual cells. Microtubules emanating from the perinuclear ncMTOC have been described as having a radial organization, and thus it is unclear that this redistribution of mCherry-Atg8a punctae to the fat body edge would reflect a kinesin-dependent process as suggested by the authors.*

Thank you for this detailed observation. Indeed, we frequently observe autophagosomes redistributing to contact-free peripheral regions upon dynein depletion, resulting in an asymmetric distribution. We believe this redistribution to be kinesin-dependent, as shown in Figure 3: kinesin overexpression scatters or shifts autophagosomes to the periphery, while kinesin/dynein double knockdown causes widespread autophagosome scattering. The simplest explanation is that, in dynein's absence, kinesins drive autophagosome movement.

Additionally, while the radial organization of the microtubule (MT) network has been documented in two independent studies that we referenced, neither study showed MT plus-ends specifically, towards which kinesins transport. It is plausible that, while the MT network appears radial and symmetrical, subtle asymmetry might influence kinesin-dependent transport in fat cells. To explore this further, we will express MT plus-end markers, such as EB1-RFP and EB1-GFP, as well as kinesin reporters like unc-104-GFP or HA-tagged kinesins.

> *(4) To validate whether the mCherry-Atg8a structures in Vps16A-depleted cells were of autophagic origin, the authors depleted Atg8a and observed a loss of mCherry- Atg8a signal from the mosaic cells (Figure S1D, J). A more rigorous experiment would be to deplete other Atg genes (not Atg8a) and examine whether these structures persist.*

Thank you for the suggestion to further validate our reporter. We will knock down additional Atg genes, including Atg14, Atg1, Atg6, and Vps34, to confirm that the mCherry-Atg8a-positive structures in the Vps16A RNAi background are indeed of autophagic origin.

> *(5) The authors found that only a subset of dynein, dynactin, rab, and rab effector depletions affected mCherry- Atg8a localization, leading to their suggestion that the most important factors involved in autophagosome motility have been identified here. However, this conclusion has the caveat that depletion efficiency was not examined in this study, and thus any conclusions about negative results should be more conservative.*

Thank you for this constructive feedback. We agree and will adjust our conclusions based on the negative results in the revised manuscript to account for the potential variability in depletion efficiency.

> ***Reviewer #3 (Public review):***
>
> *Summary:*
>
> *In multicellular organisms, autophagosomes are formed throughout the cytosol, while late endosomes/lysosomes are relatively confined in the perinuclear region. It is known that autophagosomes gain access to the lysosome-enriched region by microtubule-based trafficking. The mechanism by which autophagosomes move along microtubules remains incompletely understood. In this manuscript, Péter Lőrincz and colleagues investigated the mechanism driving the movement of nascent autophagosomes along the microtubule towards the non-centrosomal microtubule organizing center (ncMTOC) using the fly fat body as a model system. The authors took an approach whereby they examined autophagosome positioning in cells where autophagosome-lysosome fusion was inhibited by knocking down the HOPS subunit Vps16A. Despite being generated at random positions in the cytosol, autophagosomes accumulate around the nucleus when Vps16A is depleted. They then performed an RNA interference screen to identify the factors involved in autophagosome positioning. They found that the dynein-dynactin complex is required for the trafficking of autophagosomes toward ncMTOC. Dynein loss leads to the peripheral relocation of autophagosomes. They further revealed that a pair of small GTPases and their effectors, Rab7-Epg5 and Rab39-ema, are required for bidirectional autophagosome transport. Knockdown of these factors in Vps16a RNAi cells causes the scattering of autophagosomes throughout the cytosol.*
>
> *Strengths:*
>
> *The data presented in this study help us to understand the mechanism underlying the trafficking and positioning of autophagosomes.*

Thank you for your positive comment and for acknowledging the strengths of our work.

> *Major concerns:*
>
> *(1) The localization of EPG5 should be determined. The authors showed that EPG5 colocalizes with endogenous Rab7. Rab7 labels late endosomes and lysosomes. Previous studies in mammalian cells have shown that EPG5 is targeted to late endosomes/lysosomes by interacting with Rab7. EPG5 promotes the fusion of autophagosomes with late endosomes/lysosomes by directly recognizing LC3 on autophagosomes and also by facilitating the assembly of the SNARE complex for fusion. In Figure 5I, the EPG5/Rab7-colocalized vesicles are large and they are likely to be lysosomes/autolysosomes.*

Thank you for suggesting an improvement to our Epg5 localization data. We plan to perform triple-staining experiments with autophagy and lysosome markers, such as Atg8a and Lamp1, together with Epg5-9xHA to provide a clearer context for Epg5 localization.

> *(2) The experiments were performed in Vps16A RNAi KD cells. Vps16A knockdown blocks fusion of vesicles derived from the endolysosomal compartments such as fusion between lysosomes. The pleiotropic effect of Vps16A RNAi may complicate the interpretation. The authors need to verify their findings in Stx17 KO cells, as it has a relatively specific effect on the fusion of autophagosomes with late endosomes/lysosomes.*

Thank you for this valuable suggestion. We will create similar Drosophila lines as used in our study but will now employ Syntaxin17, SNAP29, or Vamp7 RNAi. We will cross our most significant hits with these new lines to confirm our findings.

> *(3) Quantification should be performed in many places such as in Figure S4D for the number of FYVE-GFP labeled endosomes and in Figures S4H and S4I for the number and size of lysosomes.*

Thank you for pointing this out, we will perform the suggested quantifications and statistics.

> *(4) In this study, the transport of autophagosomes is investigated in fly fat cells. In fat cells, a large number of large lipid droplets accumulate and the endomembrane systems are distinct from that in other cell types. The knowledge gained from this study may not apply to other cell types. This needs to be discussed.*

Thank you for this insight. We will discuss the potential cell-type specificity of our findings in the revised manuscript. Additionally, we plan to examine the distribution of the mCherry-Atg8a reporter in the vps16A RNAi background in other cell types, such as salivary gland cells, to broaden our analysis.

> *Minor concerns:*
>
> *(5) Data in some panels are of low quality. For example, the mCherry-Atg8a signal in Figure 5C is hard to see; the input bands of Dhc64c in Figure 5L are smeared.*

Thank you for noting this. We will repeat the experiment in Figure 5C to obtain clearer images. The smeared Dhc64C input bands in Figure 5L are due to the large size of this protein, which affects its migration characteristics. We will address this in the revised manuscript.

> *(6) In this study, both 3xmCherry-Atg8a and mCherry-Atg8a were used. Different reporters make it difficult to compare the results presented in different figures.*

Thank you for this comment. Both reporters are well-established as autophagic markers and function similarly. However, to reduce confusion, we have used only one type per figure to ensure comparability of results.

> *(7) The small autophagosomes presented in Figures such as in Figure 1D and 1E are not clear. Enlarged images should be presented.*

Thank you for your suggestion. We will repeat these experiments and provide higher-quality, enlarged images for clarity.

> *(8) The authors showed that Epg5-9xHA coprecipitates with the endogenous dynein motor Dhc64C. Is Rab7 required for the interaction?*

Thank you for this question. We will investigate this by co-transfecting the cells with WT and GTP- or GDP-locked Rab7 mutants (which mimic constitutively active and dominant-negative forms, respectively) with Epg5-9xHA. This will allow us to assess whether Rab7 modulates the Epg5-Dhc interaction.

> *(9) The perinuclear lysosome localization in Epg5 KD cells has no indication that Epg5 is an autophagosome-specific adaptor.*

Thank you for this comment. We will moderate our statement regarding Epg5's role as an autophagosome-specific adaptor in the revised manuscript.

https://doi.org/10.7554/eLife.102663.1.sa4